europhysicsnews

FEATURES ISSUE

34/5

2003

September/October 2003

Institutional subscription price:
91 euros per year

Euro coins and the potential risk of nickel allergy

Emergence of fuel cell products

Supercapacitors boost the fuel cell car

features

European Physical Society

EDP SCIENCES

europhysicsnews

Volume 34 Number 5
September/October 2003

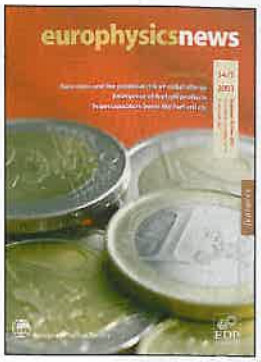

▲ PAGE 176

Fuel cells can power zero emission cars

▲ PAGE 181

the prototype of a new generation of gamma-ray detector arrays

▲ PAGE 195

The concern about nickel in coins

FEATURES

NEWS, VIEWS AND ACTIVITIES

contents

europhysicsnews

Europhysics News is the magazine of the European physics community. It is owned by the European Physical Society and produced in cooperation with EDP Sciences. The staff of EDP Sciences are involved in the production of the magazine and are not responsible for editorial content. Most contributors to Europhysics News are volunteers and their work is greatly appreciated by the Editor and the Editorial Advisory Board.
Europhysics News is also available online at: **www.europhysicsnews.com**

34/5
2003
September/October 2003
Institutional subscription price:
91 euros per year

Schedule
Six issues will be published in 2003. The magazine is distributed in the second week of January, March, May, July, September, November. A directory issue with listings of all EPS officials is published once a year.

Advertising Manager Susan Mackie
Address 250, rue Saint-Jacques, 75005 Paris, France
Tel +33 155 42 80 51
Fax +33 146 33 21 06
Email mackie@edpsciences.org

Production Manager Agnes Henri
Address EDP Sciences, 17 avenue du Hoggar, BP 112, PA de Courtabœuf, F-91944 Les Ulis Cedex A, France
Tel +33 169 18 75 75
Fax +33 169 28 84 91

Printer Rotofrance, Lognes, France

Dépôt légal: septembre 2003

Subscriptions
Individual Ordinary Members of the European Physical Society receive Europhysics News free of charge. Members of EPS National Member Societies receive Europhysics News through their society, except members of the Institute of Physics in the United Kingdom and the German Physical Society who receive a bimonthly bulletin. The following are subscription prices available through EDP Sciences. **Institutions** 91 euros (VAT included, European Union countries); 91 euros (the rest of the world). **Individuals** 58 euros (VAT included, European Union countries); 58 euros (the rest of the world). Contact subscribers@edpsciences.com or visit www.epdsciences.com

ISSN 0531-7479
ISSN 1432-1092 (electronic edition)

Emergence of fuel cell products

K. Kendall, Chemical Engineering, University of Birmigham

2003 is a crucial period for the emergence of fuel cells in products that could have far-reaching effects on our lives. Fig. 1 shows the Citaro bus that will this year make its appearance in 10 European cities as a result of the CUTE project with funding from the European Community (www.fuel-cell-bus-club.com). It is a zero emission bus driven by pressurised hydrogen gas stored in the roof space, and recharged from hydrogen filling stations especially set up for the project. The hydrogen passes into the fuel cell over a stack of proton conducting membranes and loses its electrons as it meets the platinum coated carbon electrodes coated on the anode surfaces. The hydrogen ions diffuse through the polymer electrolyte and react with oxygen on the cathode electrode, picking up electrons, again catalysed by platinum/carbon particles.

◀ **Fig. 1:** Citaro fuel cell bus.

The electrical power generated by these electrochemical reactions, around 200 kWe, drives the electric drive train of the bus, which has excellent acceleration, speed and range. The only product of the reaction is steam that can be seen exhausting from the tailpipe as the bus runs through the city streets. The catalysts were made by Johnson-Matthey, the fuel cell stack by Ballard and the bus by Daimler Chrysler.

Two other fuel cell products making their commercial debut this year (Fig. 2) are the 2003 Honda FCX car that has gained the first certification for economy and emissions in the USA (www.hyweb.de 19/02/03) and the Daimler Fuel Cell A-Class model that just won approval in Japan to be run in 60 vehicles (hyweb 13/03/2003). These again will be fuelled by 5 hydrogen filling stations being installed in Japan at the moment.

▲ **Fig. 2:** Honda FCX and Daimler Chrysler fuel cell cars.

Although these products are unlikely to replace conventional buses and cars in full commercial operations before 2020, they represent a new step towards the low emission, high efficiency hydrogen economy of the future. In addition, laptop computers, mobile phones, portable power devices, emergency back-up systems and household water heaters are all likely to be powered by fuel cells in the near term. The purpose of this article is to describe the forces pushing fuel cells into applications, to review the recent advances in technology, then to look forward to the emerging issues such as hydrogen availability and storage.

Forces driving fuel cells

First consider the major problems of our cities:-'Gloomy, noisy and dirty Birmingham' wrote Thomas de Quincy in 1849, when the city was 20 times smaller than its present dimension [1]. Although pollution was much reduced by the banning of smoky fuels in England in 1956, the emissions of barely visible NOX and particulates from cars and home heating are still substantial, while diseases like asthma, which may result from chronic exposure to irritants, are reaching epidemic proportions. It has always been necessary to legislate against technologies that emit dangerous pollutants because cleanup costs penalise the conscientious citizen. Perhaps the best example is the automobile exhaust emission legislation introduced in the US in 1969 that ultimately forced all new cars to carry exhaust catalysts, reducing CO, NOx and lead emissions considerably. This was an 'end of pipe solution' which did not fundamentally change the technical issues. But now legislation has been introduced in California to ensure that 10% of all new vehicles are 'zero emission vehicles', or ZEVs, starting in 2005 and gradually increasing to 2018. This will have a much more significant effect than the catalyst regulation because the drive train of the car must be altered in principle to accommodate this measure. Fuel cell driven cars seem to be the likeliest solution. Looking still further ahead to the end of the 21st century, it seems possible that all combustion and flame-based processes will be banned because of their harmful health consequences. Already, smoking is banned in New York public places, Hamburg has issued strong NOx limits, diesel generators are not allowed in certain locations, fires are banned in parks, etc, etc. The only logical end point is a flame-free society [2].

The second driving force for fuel cell introduction is efficiency. Although this concept is more difficult to define than pollution, because there are many different measures of efficiency, it is clear that more efficient technologies will use less fuel to achieve the same results, thus conserving our valuable fossil reserves, and utilising renewable energy more effectively. The fuel cell is the most efficient power-generating device invented so far. It converts the chemical energy of molecules like hydrogen, methane or alcohol directly into electrons at a potential near 1 Volt. Stacking a number of these cells together in series can give DC power at any desired voltage, rather like a battery of voltaic metal plates. The difference is that, unlike batteries, fuel cells do not need charging. Instead they provide power whenever fuel is pumped in. As a result, they do not need thick metal electrodes that make batteries too heavy for vehicle drives. But they share the two great advantages of batteries; high efficiencies and low emissions; advantages which our present power generation technologies do not possess.

Car engines, power station turbines and diesel generators that dominate our present culture are notoriously inefficient and dirty. Typically, only about 30% of the chemical energy in the fuel is converted into useful work by these devices because, as Carnot showed in 1824, these engines generate hot gas under pressure, and power cannot fully be extracted from a pressurised hot gas stream [3]. By contrast, a fuel cell extracts electrons directly from reacting molecules and can therefore be 100% efficient in principle. Indeed, a fuel cell can be more than 100% efficient if the reaction is endothermic and draws in extra heat energy from the surroundings, as methane does when it combines with steam. Of course, there must always be losses due to ohmic resistance and to mass transfer at the interfaces. Consequently, as more power is drawn from a fuel cell, its efficiency falls. When operating at maximum power, as in a battery, the fuel cell typically is 50% efficient since half the chemical energy is converted to external work and half to ohmic heating. Because this heat can also be converted to work

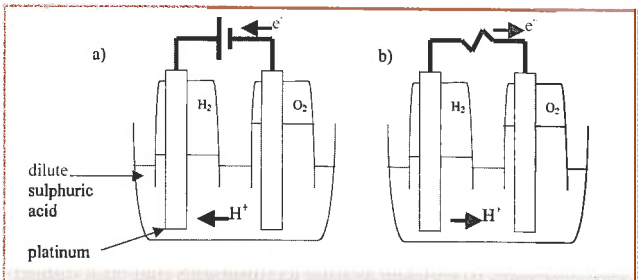

▲ Fig. 3: a) Grove's electrolysis experiment; b) Groves fuel cell demonstration.

using a gas engine, a fuel cell combined with a turbine can give an overall efficiency of 75%, as demonstrated by Siemens Westinghouse [4]. This is significantly better than a combined cycle gas turbine generator that can typically attain 50% efficiency. And whilst such combined cycle engine systems may only operate effectively at hundreds of MWe capacity, in large centralised facilities that entail high distribution costs, a fuel cell system can operate down to 1 kWe quite easily, be small enough to fit in every room and every vehicle, leading to a fully distributed power network.

In order to understand these high efficiencies, it is worth reflecting on the principle of fuel cell operation, which was originally described by William Grove in 1839. Following Alessandro Volta's invention of the battery, Grove like many scientists of his time was electrolysing water using two platinum electrodes dipped in dilute sulphuric acid to promote ionic conductivity in the solution (Fig. 3a). By passing electric current through the water-acid electrolyte, Grove generated hydrogen bubbles on one of the platinum electrodes and oxygen bubbles on the other. The two gases were kept separate by positioning individual collector vessels over each electrode. Grove's pioneering insight was to realise that the reaction was reversible. The hydrogen and oxygen can recombine at their respective electrodes to drive current in the opposite direction (Fig. 3b). What Grove recognised was that a fuel cell is an electrolyser running backwards. Just as an electrolyser can be made almost 100% efficient by operating near the equilibrium voltage, so can a fuel cell, as long as low currents and good electrocatalysts are used. Under these conditions, there are no pollutant emissions either, water being the only reaction product. More usually, it is practical to operate the fuel cell near its maximum power output, roughly half the equilibrium voltage and around 50% efficiency. But as electrical demand reduces, ohmic losses fall and efficiency rises, unlike a combustion engine that gets less efficient as it is turned down because of frictional losses.

Technology Push

So what has changed since Grove's time to make fuel cells more attractive than combustion engines? Obviously, legislation for zero emission has had the most significant effect, putting penalties in place for polluting companies. Another incentive is the climate change levy on fuels, introduced by the British Government in 2002, which has created a market for low carbon technologies [5]. Approximately 1 billion pounds will be raised by this novel tax this year, and some of that money will be used by the Carbon Trust to develop fuel cell technologies.

But the most important technical advance has been the invention of solid electrolytes to replace the nasty and messy liquids, such as sulphuric acid, used by Grove. Liquid electrolytes have a number of drawbacks; they leak, evaporate and corrode; whereas solid electrolytes are stable, non-corroding and self-supporting. Two materials are leading this advance. One is a polymer made

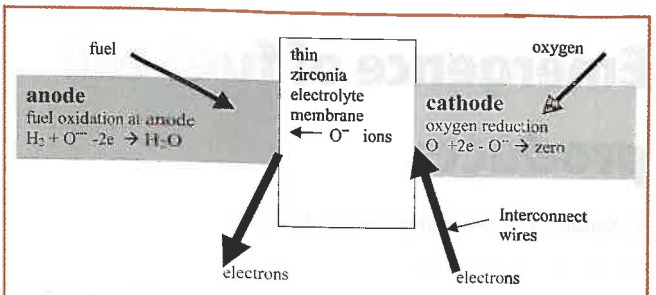

▲ Fig. 4: Operation of a solid oxide fuel cell.

from sulphonated fluoropolymer, while the other is a ceramic made from yttria stabilised zirconia.

The mode of operation is illustrated in Fig. 4 that shows that the central component of a solid electrolyte fuel cell is a thin membrane of the solid electrolyte, typically 10 to 100 μm in thickness. This allows ions to pass through but stops the flow of both gas molecules and electrons. Yttria stabilised zirconia is the simplest solid electrolyte because it only conducts oxygen ions O^-. These ions are formed by reduction of oxygen atoms that pick up electrons at the catalytic oxygen electrode (cathode) which is usually a porous lanthanum manganite semiconductor. The electrons enter the electrode through a metal wire, the 'interconnect' which connects the cell to the external circuit. The oxygen ions can then diffuse through the electrolyte membrane to the fuel electrode (anode) which is normally made of fine nickel particles supported on a porous zirconia lattice. This requires red-hot conditions, typically 800°C, for a good diffusion rate. The electrons are released from the oxygen ions and can then flow out through the interconnect wire while the oxygen reacts with the fuel, hydrogen in Fig.1, which is continually fed to the anode compartment.

The overall reaction is the sum of the two reactions occurring on the two electrodes as shown below in reaction scheme 1 for hydrogen reacting with oxygen, the simplest reaction.

Fuel electrode (anode)	$H_2 + O^- - 2e \rightarrow H_2O$
Oxygen electrode (cathode)	$O - O^- + 2e \rightarrow$ zero
Resultant overall reaction	$H_2 + O \rightarrow H_2O$

▲ Scheme 1: Two electrode reactions adding to give the complete reaction.

From this scheme it is clear that there is no product formed in the cathode compartment and only water is produced at the anode. Thus, this fuel cell is 'zero emission' as defined by US regulations. The equilibrium voltage for this reversible reaction depends on both temperature and reactant concentrations. Typically it is 1 V at 800°C. Current flow of about 1 A for each square centimetre of membrane surface is possible, and the voltage then drops because of ohmic losses to around 0.5 V. For high power, it is therefore obvious that the area of membrane needs to be as large as possible, 1 m^2 providing typically 1 kWe. Consequently, the fuel cell design must be a stack of plates or tubular cells, similar to that of a heat exchanger or a filter, devices that also depend on high membrane area for their operation.

The conclusion is that a solid state device made up of 5 layers (electrolyte + 2 electrodes + 2 interconnects) can produce DC power directly without moving parts. This is almost magical in its simplicity and lends credence to the new idea that small, reliable, efficient, zero-emission power generators may develop commercially for a number of applications in the next decade.

Applications

Already, every new car has a fuel cell built in, to control the catalyst clean-up system. This is a single cell, like that in Fig 4, comprising an yttria stabilised zirconia membrane with two electrodes and two interconnect wires, inserted in the exhaust manifold where it reaches 600 to 700°C. On one side of the membrane is air, and on the other side is the engine exhaust stream that is deficient in oxygen. The difference in oxygen concentration across the membrane creates a voltage that depends on the oxygen level. The fuel cell therefore acts as a sensor that can be used to control the engine management system for emission catalyst performance. Only a small power is required for this task, but it is envisaged in future that the whole electrical system of the car, ie the radio, electric windows, air conditioner, etc, will be powered by a stack of such cells. In the USA there is a large development project on this theme, the SECA project, supported by Siemens, Honeywell etc [6].

Of course, it is also possible to replace the whole engine of the car with a fuel cell stack, and this has now been demonstrated by many car manufacturers using the Polymer Electrolyte Membrane (PEM) fuel cell that has been much developed by Ballard in Vancouver [7]. The PEM fuel cell uses a sulphonated fluoropolymer swollen in water to conduct proton species. Carbon electrodes with platinum catalyst are pasted on each side and graphite interconnects are generally used. Humidified hydrogen is the fuel, fed to the anode compartment and air is the oxidant, which also flushes out the product water from the cathode compartment. The temperature of operation is around 100 °C. Thus this fuel cell gives zero emissions and could provide a solution to the ZEV (zero emission vehicle) legislation. Problems of hydrogen supply are still to be overcome, as are the costs of the components compared to a standard combustion engine. However, it is estimated that a significant penetration of such ZEV fuel cells will be achieved by 2020.

An alternative possibility has been demonstrated by BMW, who have used hydrogen as the vehicle fuel instead of gasoline. The hydrogen drives an almost standard internal combustion engine and also powers a fuel cell for auxiliary electricity. This satisfies ultra low emission regulations, although some nitrogen oxides are produced under combustion conditions. BMW also adopted liquid hydrogen storage, using cryostatic tanks in the trunk of the car, while proving that that these tanks could be topped up at robotic filling stations [8]. However, the practicality of such fuel storage is still in doubt.

The hydrogen storage issue is one of the most challenging problems in the fuel cell field. If the storage density is defined as the mass of hydrogen stored divided by the total mass of the storage system, then present methods, including hydrogen bottles and liquid hydrogen only give storage density of a few per cent, whereas gasoline is near 20%. Hydrides like lithium hydride (12.7% density) offer a possibility of improving over the present standard of pressurised bottles (about 5%). Carbon nanotubes have been suggested as storage media, but early reports of 50% density have not been repeatable. The currently accepted value is 0.5%. In order to evaluate the possibilities, a large European project, FUCHSIA has been started [9]. Hydrocarbons are still the best bet, if the carbon could be dealt with.

The most fundamental issue is the source of the hydrogen, which now is manufactured mainly from natural gas, but could be generated on board the vehicle from gasoline by means of a steam reformer. In this steam reacts with hydrocarbon to give hydrogen and CO. Unfortunately, such fuel processors are bulky, slow and expensive, and do not appear viable in the near future. A new approach to the hydrogen economy is needed where hydrogen is generated from renewable sources such as biogas, wind energy or photovoltaics. One possibility is methanol, derived from biomass, which can be used with a polymer fuel cell [10] to produce power for a laptop as shown in Fig. 5a. Also, natural gas is available in homes and could be used directly in the solid oxide fuel cell device [11] shown in Fig. 5b to provide both heat and power. This device was made using 1000 tubular zirconia fuel cells to replace the conventional metal burner in a water heater. In future, this could be augmented with biogas or renewable hydrogen to give a sustainable energy economy.

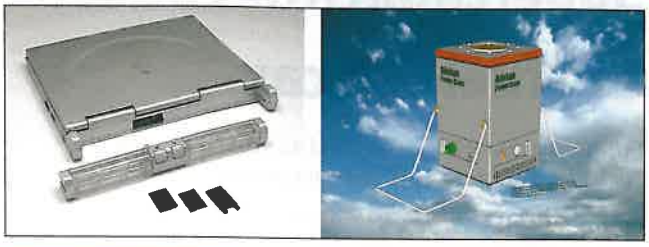

▲ **Fig. 5:** a) Casio lap-top computer powered by a PEM fuel cell fuelled by methanol; b) A solid oxide fuel cell system driven by natural gas for combined heat and power.

One exciting prospect is to generate power using such devices locally in homes. This is not yet possible with combustion engines because of their lubrication, wear, emission and ignition problems. But a small solid state fuel cell could give the reliability and lifetime needed for this application. Consider a vision of the future where each home has a fuel cell within its central heating boiler. This could run on natural gas, but also on biogas and hydrogen. Because the fuel cell is a catalytic device, without a flame, it can run on a variety of molecules, and actually runs better on diluted fuel such as biogas, whereas engines stop under these circumstances. Under base-load conditions, the fuel cell would operate at high efficiency and would also generate heat for the home. Excess power could be exported through the grid if restrictive regulations were removed. The system would be totally secure. Also, the nation's carbon dioxide emissions would be halved in the domestic and business sectors and our fuel imports reduced substantially. Totally distributed power could be achieved through fuel cells in the future. With a fuel cell in every home, there would be sufficient electricity generated without the need for large power stations.

features

References

[1] J. Paxman, The English, Penguin, London 1999, p.162

[2] K. Kendall, Hopes for a Flame-Free future, Nature 404(2000) 233-5

[3] S. Singhal & K. Kendall (eds.) Solid Oxide Fuel Cells: Fundamentals and Applications, Elsevier, Oxford 2003, ch 3

[4] J. Leeper, 220 kWe solid oxide fuel cell/microturbine generator hybrid proof of concept demonstration report, California Energy Commission, report no. P600-01-009, March 2001

[5] www.thecarbontrust.co.uk

[6] www.fossil.energy.gov/techline/tl_seca_sel1.shtml

[7] www.Ballard.com

[8] www.BMW.com/bmwe/pulse/enterprise/cleanenergy2/index.html

[9] www.bham.ac.uk/fuchsia

[10] www.casio.com

[11] www.adelan.co.uk

Fuel cells can power zero emission cars and supercapacitors help to reduce obstacles for widespread adoption of the technology

Supercapacitors boost the fuel cell car

Fritz Gassmann, Rüdiger Kötz and Alexander Wokaun
Paul Scherrer Institute, Villigen, Switzerland

No matter where you live it cannot have escaped your attention that our planet is struggling. There may be some who are sceptical but most of us can have little doubt that if we do not mend our ways, severe changes of global climate lie ahead. One of the most obvious major contributors to the deteriorating situation are the some 750 million registered vehicles worldwide that emit roughly 4 billion tons of carbon dioxide each year and contribute 15% to the anthropogenic emissions. In addition to their impact on the global climate, several other facts are motivating car manufacturers to investigate ways of reducing emissions drastically: declining oil reserves, their location in politically unstable regions, and health hazards posed by secondary emissions of nitrogen oxides, hydrocarbons, and particulates. Today's most promising solution for these problems would be cars powered by fuel cells with solar hydrogen as the ultimate energy carrier (cf preceeding article). However, a number of obstacles are delaying widespread adoption of this technology including high costs, the weight and volume of today's fuel cells, security concerns related to hydrogen storage tanks, and the missing infrastructure needed for the production and distribution of hydrogen.

All these engineering and economic problems could be minimised if cars could be built without having excessive power, e.g. a 1 ton compact-class car with 20 kW continuous mechanical power at the wheel. Imagine such a car that could reach the maximum allowed speeds in most countries (120 km/h or 75 mph), climb over every pass (it would climb 6% at a speed of 80 km/h or 50 mph) and transport people to their working places or shopping centres in the accustomed time (remember that powerful engines cannot help to lubricate a traffic jam). However, the hypothetical 20 kW car would need around 30 seconds to accelerate to 100 km/h (62 mph) and would, therefore, only be accepted by a few pioneers. The common technical answer of car manufacturers to this rather irrational but common human desire for power is oversizing engine power by a factor of about two to eight. The price customers pay for this solution is twofold: Powerful engines are more expensive, and, since these engines work below their optimum efficiency most of the time, their fuel consumption is high, causing increased operating costs and at the same time increased environmental damage.

Box 1

Physical relations for capacitors

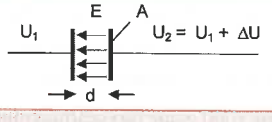

Both electrodes have a surface A (in m^2) separated by distance d (in m). The applied voltage ΔU (in Volt) creates an electric field $E = \Delta U/d$ storing the electrical energy. Capacitance C in Farad (F) and stored energy J in Ws is:

$$C = \varepsilon_0 \cdot \varepsilon_r \frac{A}{d} \qquad J = \frac{1}{2} C \cdot \Delta U^2$$

where ε_r (e.g. 1 for vacuum or 81 for water) is the relative dielectric constant which depends on the material placed between the two electrodes and $\varepsilon_0 = 8.85 \cdot 10^{-12}$ F/m is a fundamental constant.

Power reserve for 15 seconds

How do we escape from this trap? One solution is supercapacitors (also called supercaps, ultracapacitors or electrochemical double layer capacitors, EDLC) which offer the possibility for electric cars to reconcile the widespread wish for power with environmental concerns [1]. Instead of designing the primary power system to deliver a maximum of e.g. 73 kW (100 horsepower), it could be designed for an average power of only 20 kW, with supercapacitors acting as power reserves to deliver peak power during a limited time. With 53 kW of additional power delivered over 15 seconds, most power display behaviour patterns could be satisfied: The car would accelerate to 100 km/h (62 mph) in less than 15 seconds, passing other cars over short distances would be possible, and enough rubber could be burned with starts to satisfy the speedster. Additional peak power of 53 kW over 15 seconds means access to an energy buffer of 220 Wh, an amount of energy costing a few cents when taken from the electric power grid.

> Over about the last decade, double-layer capacitors with unprecedented large capacitance have been developed...

Could the *lead-acid batteries* normally employed for the electric starter motors be used for this purpose? Two main limitations must be considered. Though a normal 12 V battery with a capacity of 60 Ah stores enough energy (720 Wh), the current should not exceed about 150 A, limiting the power to 1.8 kW, far below the desired 53 kW. Secondly, chemical reactions are taking place whenever current flows into or out of a battery. In principle the transformation from bulk lead sulfate into dissolved sulfate ions is completely reversible, but the decreasing mechanical stability of the lead sulfate electrode leads to degradation after several hundred charge/discharge cycles. In spite of considerable research on new battery concepts over the last decade, no battery has been found that would circumvent these limitations.

With *capacitors* used in practically all electronic devices, e.g. to smooth ripples on the DC current in power supply units, power and stability are no problem. As energy is stored by a purely physical process in electric fields without involving chemical transformations, the number of loading cycles does not limit their lifetime. Furthermore, charge- or discharge-currents as measured in relation to the energy content, are about four decades higher

than with batteries. The big disadvantage of traditional capacitors is their relatively small capacitance. This characteristic value (measured in *Farads*) relates to their energy content when multiplied by half the square of the applied voltage (see Box *Physical relations for capacitors*). A typical large electrolyte-capacitor used for power supplies has a capacitance of the order of 20'000 micro-Farad and allows a maximum voltage of about 20 V, storing only 4 Joules of energy, equivalent to 4 Ws or 0.0011 Wh. With a mass of about 20 g for such an element, roughly 4 tons would be needed to store the required energy of 220 Wh! For an overview of frequently used capacitors in electronic devices see Fig. 1.

Supercapacitors combine advantages of battery and capacitor

Over about the last decade, double-layer capacitors with unprecedented large capacitance have been developed in various research laboratories, and several companies have already started commercial production. At the Paul Scherrer Institute in Villigen, Switzerland, Rüdiger Kötz and his group have developed an electrode in collaboration with the Swiss company *montena* (recently merged with *Maxwell*). Towards the end of 2001, one of their supercapacitors reached a capacitance of 1600 Farad at a maximum voltage of 2.5 V. They store 5000 Joules or 1.4 Wh within a volume of roughly 0.3 L (5 cm diameter, 14 cm long) weighing 320 g. To store the required 220 Wh, 160 supercapacitors weighing 50 kg would suffice. With their small internal series resistance of 0.0014 Ohm, they can produce or absorb peak currents of over 300 A. Due to the excessively high currents at low voltages, operation is normally restricted to between 50% and 100% of maximum voltage and therefore, only 75% of the energy capacity is used (due to the quadratic relationship between voltage and energy content, the residual energy equates to only 25% at 50% of the voltage). This restriction and also losses in power converters result in increasing the number needed from 160 to about 250 supercapacitors, weighing nearly 100 kg, including cables and electronics.

How to build a large capacitor?

In a capacitor, energy is stored within the electric field between its electrodes in the following way: The application of a voltage between the electrodes results in the flow of electrons towards the negative electrode, and away from the positive electrode (see Box *Physical relations for capacitors*). This transport of electric charge towards and from the respective electrodes is equivalent to an electric current. Multiplication of this current by the applied voltage gives the power flowing into the electric field between the electrodes. The capacitance is determined by the geometric dimensions of the device and by the relative dielectric constant of the applied isolator foil. While this latter value lies between 1 for air to 81 for water and up to several 1000 for ceramics, more can be achieved by manipulating the geometry. Capacitance is proportional to the surface area of the electrodes divided by their separation distance, giving units of length (at the beginning of radio telecommunication, capacitors were therefore measured in cm). Simple capacitors consisting of two parallel plates reach only very small capacitances, of the order of pico-Farad ($1pF = 10^{-12}$ F), and are used in high frequency technology. Even when loaded to 1000 V, the energy content of such *plate capacitors* is only of the order of micro-Ws (see lowest picture in Fig. 1).

To increase the geometrical part of the capacitance, the surface area of the electrodes can be increased by rolling long stripes of conducting material, and at the same time, the isolating layer of material with high dielectric constant in between them is manufactured as thin as possible. With this technology, *rolled capacitors* of the order of 0.1 micro-Farad ($1\ \mu F = 10^{-6}$ F) resisting voltages up to about 1000 V can be produced, storing around 0.05 Ws of energy (see second lowest picture in Fig. 1).

▼ **Fig. 1:** Capacitors covering a range of 15 decades.

Capacitance in Farad	1000	$1{\cdot}10^{-3}$	$1{\cdot}10^{-6}$	$1{\cdot}10^{-9}$	$1{\cdot}10^{-12}$
Example	 supercapacitor with 1500 F, max. 2.5 V (positive electrode left)	 electrolyte capacitor with 1000 mF, max. 25 V (positive electrode left)	 electrolyte capacitor with 10 mF, max. 35 V (bent wire is positive electrode)	 rolled capacitor with 51 nF, max. 63 V	 plate capacitors with 50 pF. Left: an element from an old vacuum-tube radio in the form of two plates rolled to a cylinder, max. 450 V. Right: modern ceramic element, max. 100 V)
Energy Stored	Watt hours (Wh)	several Ws (Ws)	milli-Ws = 10^{-3} Ws (mWs)	milli-Ws = 10^{-3} Ws (mWs)	micro-Ws = 10^{-6} Ws (mWs)
Applications	Novel applications in power electronics: e.g. in cars, for replacing batteries in consumer electronics	Power supply units	Low frequency technology: general electronics, e.g. audio amplifiers	Low frequency technology: general electronics, e.g. audio amplifiers	High frequency technology: e.g. radio, TV, PC

Another possible way to increase the geometrical part of the capacitance is to replace one of the electrodes by a liquid electrolyte (an electrically conducting gel) in order to achieve immediate geometrical contact on the atomic scale to the surface of a metallic electrode. A thin oxidic layer on the surface of the metal electrode serves as an isolator and separates the electrodes to distances of the order of nanometres, pushing capacitance into the tens of milli-Farad range (1 mF = 10^{-3} F) at maximum voltages of around 20-40 V. These so called *electrolyte capacitors* can store up to several Ws of energy (see middle and second highest picture in Fig. 1).

Increasing the surface area by rolling and minimizing the separation distance to the molecular range long seemed the ultimate limit in the production of large capacitors. However, *fractal geometry* has opened amazing, and counterintuitive, new possibilities of how to scramble e.g. the surface of a football-field into a 1 mm thick layer above a sheet of paper the size of the journal you are reading right now. By increasing the electrode surface about 100'000-fold in this way, electrolyte capacitors with thousands of Farad can be built.

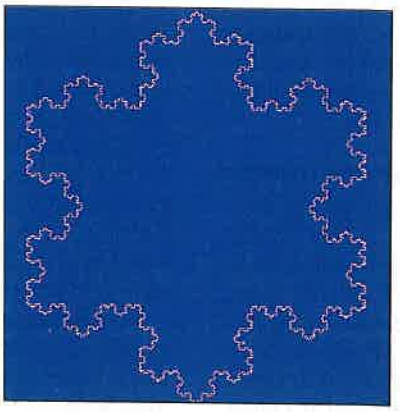

▲ **Image:** The *Kock island*.

The mystery of the inner surface

Back at the beginning of the 20th century, "mathematical monsters" were invented: by an iterative process involving ever smaller lengths, linear objects with infinite length were created which could be fitted into a limited area, that was not at all filled up by the object. One of the most famous of these objects is the curve invented by the Swedish mathematician N.F.H von Koch in 1906: A line of unit length is divided into three equal parts, the middle segment being replaced by two lines of length one third each. Obviously, repeated iteration leads to an ever longer path, because its length is multiplied by 4/3 with every iteration. On the other hand, the resulting line never exceeds a square of unit side length, nor does it need a considerable fraction of the square, because even a very long mathematical line still has zero surface. However, more and more points on the line are located close to an increasing number of points belonging to the surface of the square, yet eyeball inspection gives the impression that the geometrical object somehow combines the characteristics of a line and of a surface. With fractal dimension D, this qualitative property is put into an objective mathematical framework (see Box: *Fractal Dimension*).

Applying fractal geometry to increase the capacity [4], the surface of the electrodes has been roughened by using soot particles in contact with the flat metallic carrier-foil of the electrode (see Fig. 2a: micrograph of cross section). A measurement of the fractal dimension of the borderline in a cross-section perpendicular to the electrode yields D ≈ 1.6 (see Fig. 2b,c,d). Using a general topological formula yields $D_S \approx 2.6$ for the overall dimension of the electrode surface. As self similarity of every physical object is limited to a maximum range between its macroscopic and the atomic scale, the concept of fractal dimension is also restricted to a limited range of length scales. Considering $D_S \approx 2.6$ as representative between the macroscopic scale of the electrode (of the order of 0.1 m) and the microscopic scale (in the order of 1 nm), self similarity can be assumed to hold over 8 decades. The electrode surface is therefore multiplied by 10 to the power of 8*(2.6-2) or 60'000. In combination with the extremely thin electro-chemical double layer (around 1 nm), unprecedented capacitances can be reached.

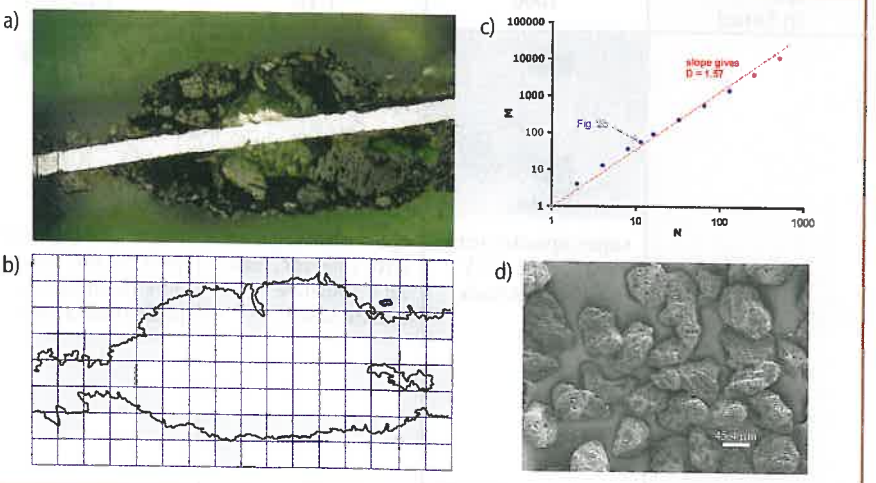

▶ **Fig. 2:** Measurement of the fractal dimension of the electrode surface.
a) Micrograph of a cross section through a supercapacitor electrode. The white stripe is a part of the 30 µm thick metallic carrier-foil (total foil is 0.1 m wide, 2 m long). On both sides carbon particles provide a complex fractal surface responsible for the high capacity. The space taken by the green resin used to fix the delicate carbon structure before cutting and to provide a good contrast for imaging is normally filled with the electrolyte (an organic solvent containing salt ions).
b) Borderline of the cross section through the electrode surface in (a) to be analyzed by the box-counting procedure, illustrated for a tiling with 128 squares: M = 56 squares (filled with light blue colour) are necessary to cover the borderline. Their side lengths are N = 11.3 (square root of 128) times smaller than the length scale of the whole picture.
c) The box-counting procedure is repeated with a computer program for different N. The average fractal dimension of the borderline is the gradient of the straight line approximating the measured points in this Log(M) over Log(N) plot, giving D ≈ 1.6. This same dimension was measured in the length-interval covering nearly 3 decades between 0.6 mm (length of micrograph in Figs 2a, b) and about 1 µm (fine structure in Fig. 2d).
d) Carbon particles as seen with an electron microscope show roughness also in the 1 µm scale. It is assumed that the above indicated fractal dimension D holds over the entire range of 8 decades between the macroscopic scale (i.e. the geometric size of the order of 0.1 m) and the microscopic scale (i.e. the micro-pores in the order of 1 nm = $1 \cdot 10^{-9}$ m). The electrode surface is therefore multiplied by $10^{8*0.6}$ or about 60'000 when compared to the normal two-dimensional surface of 0.2 m^2.

▲ **Fig. 3:** Module with 142 supercapacitors and electronics for voltage balancing that was placed under the hood of the *Hy.Power*. A similar module with 140 supercapacitors was placed below the rear seats.

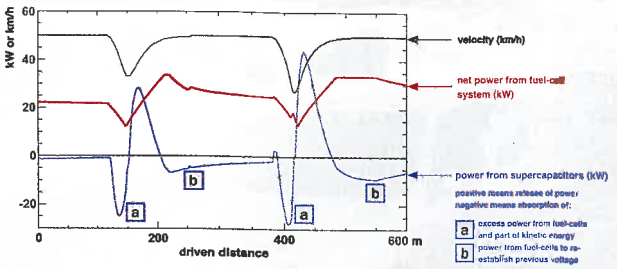

▲ **Fig. 4:** Simulation of power flows for an uphill drive on a steep mountain road through a typical double-curve. In both curves, velocity has to be reduced from 50 to about 30 km/h (black curve). The net power of the fuel cell system is regulated with maximum gradients of 3 kW/s (red curve). Excess power of the fuel cells and braking energy is stored in the supercapacitors (blue curve, large negative swings marked (a)). Accelerating after the curves is based mainly on supercapacitor power (large positive swings). After the acceleration phases, the supercapacitor system is refilled with energy from the fuel cells (smaller negative swings marked (b)).

Power box for an electric car

To demonstrate the practicability of using supercapacitors to power a car, two modules were assembled with 140 and 142 supercapacitors (Fig. 3 shows one of them) developed in the framework of a collaboration between the Paul Scherrer Institute and the company *montena* SA in Rossens, Switzerland. This capacitor bank is capable of delivering 50 kW over 15 seconds. We arranged the 282 supercapacitors in pairs of elements connected in parallel. These pairs were then connected in series, leading to a voltage range between about 175 and 350 V, with each element operating between 1.25 and 2.5 V. When starting with fully loaded supercapacitors, the current is 150 A, supplying a power of 50 kW, and this increases to 300 A at the lower bound of operation voltage. As current is distributed between two supercapacitors connected in parallel, only half of the current flows through each element, far below the maximum ratings. The voltage range 175-350 V for this arrangement is favourable for further processing in a DC/DC power converter, developed by the Swiss Federal Institute of Technology (ETH) in Zürich, that transforms the voltage to a stabilized value. However, the series connection of a large number of capacitor pairs resulted in a problem: Small differences in the characteristics of the individual elements lead to different self-discharge rates (without involving external current), resulting in steadily growing asymmetries between the voltages across different pairs of supercapacitors. As the maximum voltage of 2.5 V must not be exceeded, charge asymmetries have to be eliminated by redistribution between neighbouring pairs of capacitors. This task was accomplished by electronics specially developed for this purpose by ETH Lausanne, Switzerland.

The introduction of supercapacitors for use as a power buffer demands advanced power management that properly directs the energy flows. Instead of a direct coupling between the gas pedal and the fuel supply, an intelligent controller was developed by Paul Rodatz at ETH Zürich that translates a power demand (deduced from the position of the gas and brake pedals) into energy flows from the fuel cells, from the supercapacitors or from both systems into the driving engine. Conversely, during braking, power is taken from the engine, serving as an electric generator, and is fed into the supercapacitors. For various US and European mixed driving cycles, it has been shown that fuel consumption can be cut by 5-15% due to this regenerative mode of braking. The supercapacitor voltage is regulated based on a strategy adapted to the driving situation: At low speeds, the supercapacitors should be

features

Box 2

Fractal Dimension

Assume a first measurement process performed with a stick of unit length. Obviously, it can be placed exactly once over the curve, and its finer structures are not detected. By repeating the measuring process with a measuring stick three times shorter than before (N = 3), it can be placed four times (M = 4) onto the "Koch curve". The same reasoning holds for any successive refinement of the measurement process. Consider now the well known definition $M = N^D$, holding for all smooth geometrical objects, giving D=0 (point), D=1 (line), D=2 (area) or D=3 (cube) when measured with successively smaller length scales. Applying the same definition for the "Koch curve" with N=3 and M=4 leads to a "fractal" dimension $D = (\log 4)/(\log 3) \approx 1.2618$. Over recent decades the concept of fractal dimension found numerous interesting applications in such diverse fields as geology, ecology, cosmology, physics and chemistry, medical sciences and economics [2, 3].

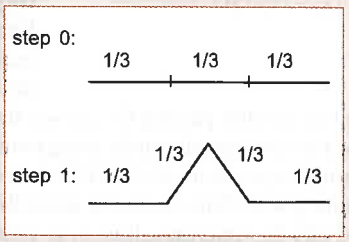

Step 0: Line of unit length is divided into 3 equal intervals.

Step 1: The central interval is replaced by two lines of length 1/3, so increasing total length of the object by a factor of 4/3 = 1.3333.

For the next step, the procedure is repeated for all four intervals, and so on. With an increasing number of iterations n, the length of the line gets therefore 1.3333^n and so exceeds every arbitrary large number, i.e. its length diverges towards infinity. A similar procedure leads to the well known *Koch snowflake* or *Koch island* (see picture).

▲ **Fig. 5:** *Hy.Power* arriving on the 2005 m (6580 ft.) high Simplon pass in January 16, 2002 during harsh weather conditions.

nearly full to offer enough energy for acceleration, while near maximum speed, supercapacitor voltage should be low, providing enough capacity for recovery of kinetic energy during braking. As an additional facet, capacitors should be nearly full during uphill-driving independent of speed, to guarantee a power reserve for steeper sections of the road. Obviously, the supercapacitors should be loaded only when power reserves are available from the fuel cell system. A simulation of power management for driving along an uphill S-curve of a mountain road is shown in Fig. 4. Just before entering the curves, velocity is reduced from 50 km/h (30 mph) to about 30 km/h (20 mph). At the same time, the power of the fuel cell system is reduced at a rate of 3 kW/s (though the electrochemistry in fuel cells works on a time scale of milliseconds, the distribution of air and hydrogen is a much slower process limiting the rates of variation of power). The excess power from the fuel cells not needed for traction, together with a part of the kinetic energy, flows into the supercapacitors (negative swing of supercapacitor power in Fig. 4). After passing the curves, the car is again accelerated to the previous speed, mainly using power from the supercapacitors (positive peaks of 30-50 kW). As soon as the fuel cells deliver more power than needed to drive the car, their excess power is fed into the supercapacitors to re-establish their previous state of charge (90% of maximum capacity).

The introduction of supercapacitors for use as a power buffer demands advanced power management that properly directs the energy flows.

A test on the road

To understand the absolute power levels, an experimental platform termed *Hy.Power* was realized by an interdisciplinary team headed by Philipp Dietrich [5-7]. It was based on a Volkswagen BORA chassis and body equipped with an electric engine and the fuel cell power train. From the designed 48 kW maximum power output of the module consisting of six PEM fuel cell stacks (PEM = Polymer Electrolyte Membrane), about 20% is needed for auxiliaries. The most energy intensive auxiliary is the compressor providing air at a pressure of about 2 bar (1 atmosphere overpressure), to ensure oxygen flow through the 0.3 mm deep channels of the bipolar stacking plates, which distribute the air across the surface (200 cm^2) of the electrodes. At the other electrode, separated from the former by the PEM membrane, hydrogen is supplied from two 350 bar pressure tanks of 26 L each. In the fuel cell reaction, oxygen and hydrogen are combined to water, and water vapour is the only exhaust of this zero emission vehicle. With a total of 1.1 kg of hydrogen stored in these tanks, the *Hy.Power* car would run over about 50-100 km (simulated for different driving cycles).

As one of the tests for our *Hy.Power* car, the 2005 m (6580 ft.) high Simplon pass connecting Brig (680 m (2230 ft.), Switzerland) with Domodossola (Italy) was chosen. Both with regard to energy and power, the requirements of this test route were about three times more stringent than those of other test runs previously completed by fuel cell vehicles. Not surprisingly Philipp Dietrich and his group experienced extremely hard days and even harder nights to prepare this real world test! During the cold morning of January 16, 2002 (-9°C, 15°F), the long-expected event took place. The relief on every face was clearly evident when the *Hy.Power* came round the last curve and arrived on the snowy Simplon pass (see Fig. 5).

References

[1] R. Kötz and M. Carlen, *Principles and applications of electrochemical capacitors*, Electrochimica Acta **45**, 2483-2498 (2000).

[2] B.B. Mandelbrot, *Gaussian Self-Affinity and Fractals*, Springer, New York, Berlin, Heidelberg (2002).

[3] H.M. Hastings and G. Sugihara, Fractals — A user's guide for natural sciences, Oxford University Press (1993).

[4] R. Richner, S. Müller, M. Bärtschi, R. Kötz and A. Wokaun, *Physically and Chemically Bonded Material for Double-Layer Capacitor Applications*, New Materials for Electrochemical Systems **5**(3), 297-304 (2002).

[5] P. Dietrich, F. Büchi, A. Tsukada, M. Bärtschi, R. Kötz, G.G. Scherer, P. Rodatz, O. Garcia, M. Ruge, M. Wollenberg, P. Lück, A. Wiartalla, C. Schönfelder, A. Schneuwly and P. Barrade, *Hy.Power — A Technology Platform Combining a Fuel Cell System and a Supercapacitor Short Time Energy Storage Device*, proc. SATG Konferenz 13.9.02, Will (2002).

[6] P. Dietrich, F. Büchi, A. Tsukada, M. Bärtschi, R. Kötz, G.G. Scherer, P. Rodatz, O. Garcia, M. Ruge, M. Wollenberg, P. Lück, A. Wiartalla, C. Schönfelder, A. Schneuwly and P. Barrade, *First Results of the Hy.Power — A Hybrid Fuel Cell Powertrain with a Supercap Energy Storage Device*, proc. VDI-Konferenz 24.-25.10.02, Dresden (2002).

[7] P. Rodatz, O. Garcia, L. Guzzella, F. Büchi, M. Bärtschi, A. Tsukada, P. Dietrich, R. Kötz, G.G. Scherer and A. Wokaun, *Performance and operational characteristics of a hybrid vehicle powered by fuel cells and supercapacitors*, Soc. of Automotive Engineers, SAE paper 2003-01-0418 (2003).

The EUROBALL gamma ray detector array

G. de Angelis[1], A. Bracco[2] and D. Curien[3]
[1] Istituto Nazionale di Fisica Nucleare, Laboratori Nazionali di Legnaro, Legnaro, Italy
[2] Dipartimento di Fisica dell'Universita' and Istituto Nazionale di Fisica Nucleare, Sezione di Milano, Milano, Italy
[3] Institut de Recherches Subatomiques, Strasbourg, France

THE EUROBALL collaboration is a common effort of several European countries to provide a forefront experimental facility for nuclear structure research. Using composite germanium (Ge) counters, the EUROBALL detector is the prototype of a new generation of gamma-ray detector arrays that has set new limits to gamma-detector technology and provided a step forward both in basic research and in applications. As an example of application outside the nuclear physics domain we should mention the recent discovery by the NASA probe, Mars Odyssey, of large quantities of hydrogen that most probably is bound in water under the Mars surface. This evidence was obtained through neutron and gamma detection, the latter based on the EUROBALL detector technology (encapsulated γ-ray detectors)—see Fig.1 [1].

The Euroball array consists of 239 Ge crystals geometrically arranged in order to cover 45 % of the total solid angle. Technical details are reported in ref. [2]. Installed at two of the main nuclear structure facilities in Europe, at LNL (Legnaro-Italy) and at IReS-Vivitron (Strasbourg-France), see fig. 2, it has allowed the investigation of atomic nuclei at extreme conditions of angular momentum values and of proton/neutron ratios.

This paper will give an overview of the research activities by selecting a number of examples. We, the authors, would like to dedicate this article to the memory of our IReS colleague and good friend Dr. Jean-Pierre Vivien who has untimely and brutally passed away when this paper was under discussion.

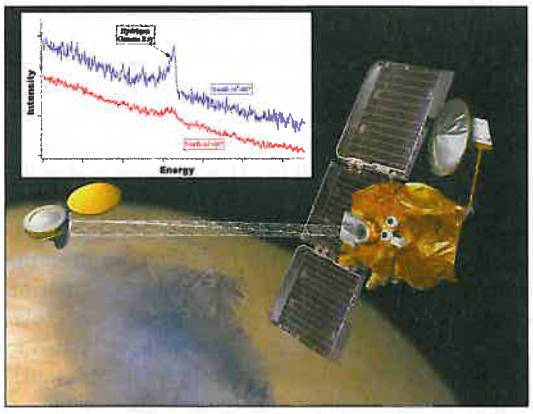

▲ Fig. 1: Mapping elements through γ-ray detection using the Mars Odyssey satellite. Neutrons and γ-rays are produced by the interaction of cosmic rays on Mars. The inset is a portion of the Odyssey γ spectra showing the emission line due to the capture of thermal neutrons by hydrogen. The γ counter uses the incapsulation technology developed for EUROBALL.

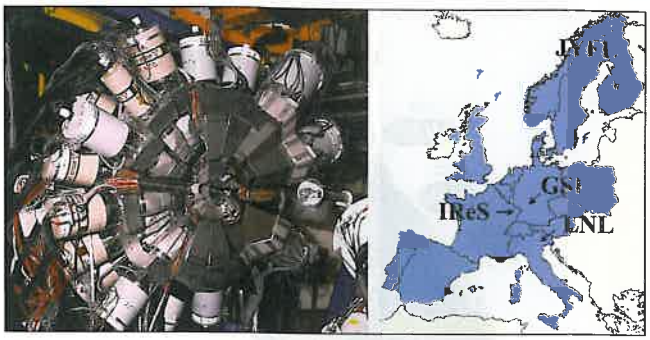

▲ Fig. 2: The EUROBALL gamma ray detector array, presently at IReS (F), has been previously operated at LNL (I). Parts of the detector will be reassembled at GSI (D) for being used with beams of radioactive ions (RISING project) and at LNL (I) coupled to a magnetic spectrometer (PRISMA) to exploit the high intensity stable beams provided by the accelerator complex of the laboratory. The remaining detectors will move to JYFL, Jyväskylä (Finland) to complement the Jurogam array.

Why study nuclei at extreme conditions?

The atomic nucleus is the paradigm of a mesoscopic system (finite many-body system) of strongly interacting Fermions where quantal size effects play a central role. Renormalization effects for the nucleon-nucleon interaction are strongly boosted by making the system more polarizable, that is less bound. A detailed investigation of the nuclear structure of nuclei at extreme conditions, both at the limit of angular momentum and of isotopic spin (neutron/proton ratio) where specific parts of the nuclear forces are strongly amplified, allows definitive tests to be carried out on the effective interaction acting between nucleons in nuclei. These studies provide the basis for a first principle description of the nuclear structure and are necessary to set stringent limits on fundamental symmetry-violation effects and on the lifetimes of rare processes. With an experimental sensitivity up to 10^{-5} of the production cross section, such as that of Euroball, it has been possible to provide an unprecedented study of the nuclear properties under extreme conditions by addressing a number of problems concerning high spins and nuclei far from stability.

Nuclear Structure at the limits of the angular momentum

Through the response of the nucleus to rotational stress one can investigate a wide variety of nuclear structure phenomena showing the different facets of a finite fermionic system. In spite of the fact that rotating nuclei have been studied since the early 50's, many new phenomena have been encountered and open questions still remain in this field. Particularly intriguing is the existence of very elongated nuclear shapes and the appearance of new degrees of freedom (unusual symmetries like tetrahedral or octahedral) [3].

The stabilization of very exotic shapes at high angular momentum not only provides unique information on the detailed structure of the nuclear potential but also allows one to infer the underlying symmetries characterizing the dynamical system. Breaking of the rotational symmetry can be related to asymmetries in charge distribution (related to deformed shapes as for macroscopic objects) or to current (only quantal) distribution. The most common are prolate elongated axial-symmetric shapes. Prolate axial-symmetric structures with approximately 2:1 and 3:1 axis ratios are called super- (SD) and hyper- (HD) deformed—see figure 3. For these highly deformed structures,

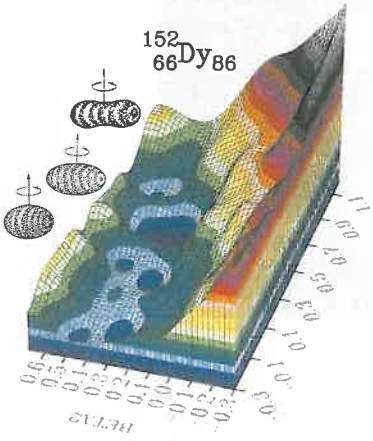

▲ Fig. 3: Potential energy surface as a function of the quadrupole deformation, (β_2 cos(30+γ)) and (β_2 sin (30+γ)), calculated for the very elongated structures in ^{152}Dy. One notices the very pronounced minima corresponding to superdeformed (SD) and hyperdeformed (HD) shapes coexisting with the normal deformed (ND) shape of the nucleus.

information on the properties and the behavior of the nucleus is contained in a cascade of about thirty gamma-rays emitted as it de-excites to its ground state from the highly excited state in which it was produced. With the EUROBALL array, designed to pick out high multiplicity cascades of γ-rays, discrete nuclear states up to the fission limit have been identified. Beyond the region of discrete states, studies of the high-spin quasi-continuum have brought information on the order-chaos transitions. In particular, in connection with superdeformation, which has become one of the areas at the forefront in nuclear structure, the problems of the feeding and decay-out of the SD bands have attracted particular interest. Concerning the problem of the feeding of superdeformed configurations, it is important to mention that indications on the γ-decay of the giant dipole resonance built on SD excited states have been recently obtained [4]. Below we describe in more detail results showing the first evidence for non-axially-symmetric superdeformed shapes and the status for the search for hyperdeformation.

Triaxiality and wobbling motion

Nuclei when rotating may also develop shapes in which the axial symmetry is broken [5]. In contrast to the region around the ground states where deformed nuclei are known to be of axial-symmetric quadrupole type, at high spin, because of the effect of the Coriolis and centrifugal forces, one expects a considerable deviation from the axial-symmetric shapes—see figure 4. In principle any elongated nucleus can be treated as a quantum rotor that can be brought into rotational motion in a nuclear reaction. In a quantum description only discrete energy values can be associated with the rotational motion, the lowest energy usually corresponding to the most regular rotation. For an even-even elongated nucleus such a rotation corresponds to the direction of angular momentum that is perpendicular to the geometrical elongation axis. Any further intrinsic excitation of the system must lead to a perturbation of such a regularity and in particular some excited individual-nucleons that tend to align their angular momenta with the axis of collective rotation R will necessarily influence the original regularity of the motion: the regularity will be lost. A classical image of such a situation is known from the

◀ Fig. 4: Pictorial representation of a triaxial nucleus: a shape like a kiwi fruit.

studies of the rigid top that, under specific initial conditions, produces characteristic precession phenomena. Generally one may associate the word "wobbling" with the forms of the motion accompanying such excitations.

It represents a small amplitude fluctuation of the rotational axis away from the principal axis such as a precession motion with the largest moment of inertia, which translates into the "zigzag" pattern of the gamma transition probabilities. This wobbling mode is similar to another collective mode—the γ vibration—associated with the transition from an axially symmetric to a triaxial mean field in the non-rotating case. Excitations of the wobbling mode was predicted long ago and have recently been identified due to the high sensitivity of EUROBALL [6,7].

Search for hyperdeformation

The nuclear many-body system may, under the influence of rotational induced forces, develop various exotic shapes. Most appealing is the strongly elongated, axially symmetric hyperdeformed (HD) shape with principal axis ratio 3:1, which is predicted in different regions but is still not fully experimentally identified. Much emphasis has been devoted to studies of the interplay between reaction dynamics, binding energies and fission barriers to optimize the population of HD structures at the limits of reachable angular momentum. Nuclei in mass regions where experiments are ongoing are Ba, Xe and Sn. Traces of structures in the decay pattern which are presumably generated by nuclei of very elongated shapes were recently observed-see Fig. 5.

In figure 5 an energy matrix of γ–γ coincidences is sliced on a plane orthogonal to the main diagonal. In such a representation γ-ray cascades with a definite moment of inertia appear as a pair of energy peaks equally spaced (modulus an integer number) with respect to the main diagonal (ridge structure). The distance between such peaks (shown by the arrows and corresponding to 2nW equal to 105 (n=1), or to 210 (n=2), is proportional to the moment of inertia (here $J \sim 75\ \hbar^2 MeV^{-1}$). Such a value of the moment of inertia corresponds to a 3:1 axis ratio. Ongoing experimental work is expected to clarify better the existence and nature of these structures. In fact, the problem of hyperdeformation remains open also in view of the fact that another possible explanation for the observed weak ridge structure could be related to an oblate-prolate phase shape transition (called a Jacobi transition) predicted by the liquid drop model at the highest spins.

Cluster and molecular structures in nuclei

Very elongated shapes are also predicted in light nuclei. The most exotic examples involve α-particles and ^{12}C or ^{16}O clusters as substructures. The existence of cluster deformed shapes is deduced mainly from the observation, in light symmetric systems, of resonances in binary reaction channels. Such molecular structures

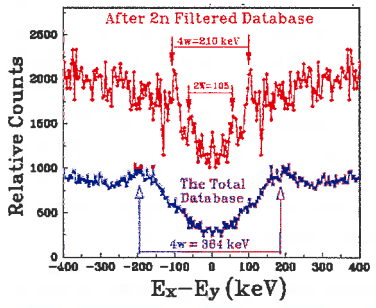

▲ **Fig. 5:** Gamma spectra of ^{126}Ba obtained requiring coincidences of equally spaced gamma-rays (Ex-Ey=k). The presence of peaks in the red top spectrum, after filtering on high-fold events, is here a signature of rotational structures with constant moment of inertia. The moment of inertia can be deduced by the energy separation of the pairs of peaks. It is compatible with a 3:1 axis ratio and is a possible indication of HD structure at high angular momentum.

also give rise to exotic shapes like reflection asymmetric molecular structures and to strongly deformed isomeric states consisting of clusters and loosely bound neutrons in multi-centre orbits [8].

Breaking the rotational symmetry by current distributions

Until recently it was thought that near-spherical nuclei always emitted irregular patterns of γ-rays. However, very regular patterns in the energies of γ-ray cascades—and hence possible evidence for rotation—were detected in nuclei that were known to be almost perfect spheres [9]. For these cases most of the angular momentum of the nucleus is generated by just a few of the valence protons and neutrons, whose coupling is governed by the overlap of the wave-functions that represent the distribution of nucleon density in the nucleus. Their configuration can be thought of as an unisotropic arrangement of crossed "current" loops embedded in the spherical mass distribution of the nucleus—figure 6. An orientation axis is defined along the total angular momentum vector, J, and the system can rotate about this axis. This behavior, investigated also at the EUROBALL spectrometer [10], has been termed "magnetic rotation" because the rotational sequences of states (and transitions) arise from the anisotropy of currents in the nucleus, which produce a magnetic moment [11]. In comparison, the more familiar rotation of deformed nuclei (and molecules) could be named "electric rotation" to reflect the fact that it results from an anisotropy in the charge (and mass) distribution.

A related topic is the spontaneous chiral symmetry breaking (giving rise to left- and right-handed systems as in molecules) which has been discovered in odd-odd nuclei having triaxial shapes. It is based on the fact that three spatial orientations are different, namely configurations where the angular momentum vectors, i) of the valence proton, ii) of the valence neutron and iii) of the core rotation, are mutually perpendicular. Such angular momentum vectors can form a left- and a right-handed system, related by the chiral operator, which combines time reversal and rotation by 180 degree. Spontaneous chiral symmetry breaking in the body-fixed frame is manifested in the laboratory frame as almost degenerate doublets of gamma transitions in ΔI=1 (P=1) bands—see right hand side of figure 6.

Nuclear Structure at the limits of the isotopic spin

The most critical quantities in determining the predicted properties of a nucleus from a given effective interaction, is the overall number of nucleons and the ratio N/Z of neutrons to protons. It is the extremes in these quantities, which define the limits of existence for nuclear matter. This new field of research in nuclear physics will be opened up by the second generation radioactive beam accelerators. In the case of nuclei not too far away from the valley of stability, there is the possibility to investigate them using high intensity beams of stable ions in combination with very efficient detectors. A large part of the EUROBALL experimental program has been dedicated to the investigation of the structure of proton-rich nuclei through a large variety of dedicated ancillary detectors for reaction products.

Selfconjugate nuclei and mirror symmetries

Isospin symmetry is a consequence of the approximate charge invariance of the nucleon—nucleon forces. The isospin symmetry explains the nearly identical energy spectra observed in pairs of mirror nuclei. The main contribution to the isospin symmetry breaking is the Coulomb interaction. Although the symmetry is already broken to some extent, at the level of the strong interaction, and to a much larger extent by electromagnetic forces, the isospin formalism remains a very powerful tool.

Isospin symmetry allows one to relate the properties of corresponding levels in different nuclei, from which complementary information can be derived on the structure of the nuclear wave function. The energy differences of analog states along rotational bands in mirror nuclei—mirror energy difference (MED)—have been investigated in the last few years in the $f_{7/2}$-shell in the mass region between A = 40-60 and for heavier nuclei. By resorting to large scale shell model calculations the mechanism of the back-

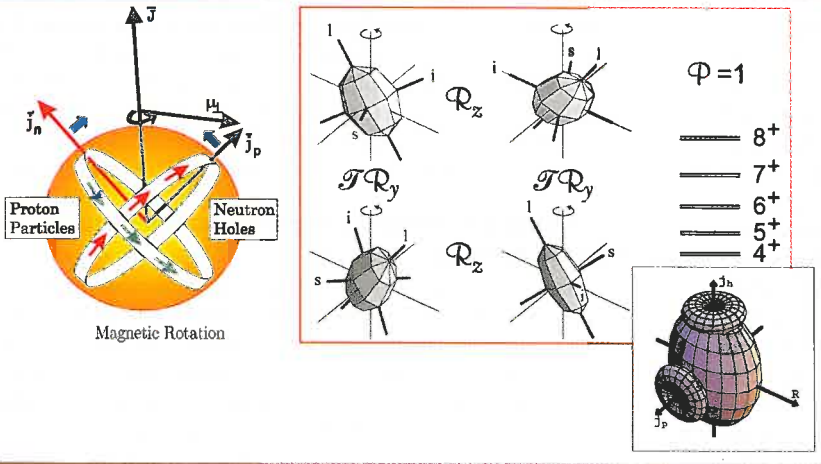

◀ **Fig. 6:** *(Left)* crossed current loops generated by proton particles and neutron hole configurations. The breaking of the rotational symmetry of the nucleus by such unisotropic current distributions appears through regular rotation-like gamma spectra. *(Right)* Pictorial view of a triaxial nucleus showing the symmetry operation (P) related to chiral symmetry breaking, time reversal (T) and finite rotation (R), which result in a doublet splitting (same spin and parities) of the rotational states. The inset depicts orbitals of a high-j proton particle and a high-j neutron hole coupled to the triaxial density distribution. (picture by courtesy of S. Frauendorf.)

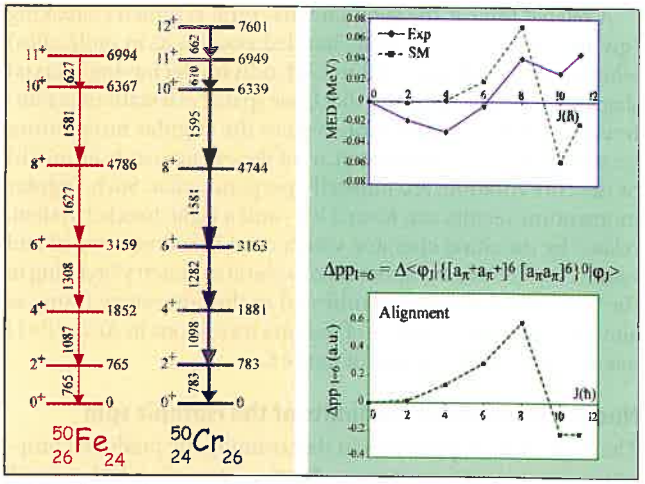

▲ **Fig. 7:** *(Left)* excited states of ^{50}Fe -^{50}Cr mirror nuclei investigated with EUROBALL. *(Right)* The upper part of the figure shows the measured (Exp) and calculated (SM) energy differences for mirror nuclei as a function of the angular momentum. The maximum of the curve indicates an alignment process of a pair of nucleons. The lower part of the figure shows the average number of proton pairs in the maximal aligned configuration (by Shell Model calculations).

bending in rotating mirror nuclei has been related to the MED and explained in terms of the alignment of like-nucleon pairs—see figure 7. It has also been shown that the MED gives information on the evolution of nuclear radii along the yrast bands and provides direct evidence for charge-symmetry breaking of the nuclear field [12].

Isospin Symmetry

The consistency of the standard model for electro-weak interaction can be checked through the unitarity test of the Cabibbo-Kobayashi-Maskawa (CMK) matrix. New data, based on super-allowed Fermi β-decay rates, suggest that the CMK-matrix fails the unitarity test, pointing to physics beyond the Standard Model. These conclusions partly rely on calculations of the corrections for nuclear isospin purity of heavy N=Z nuclei. The size of the isospin mixing in low energy nuclear states has recently been determined in the mass A≈60 region through the precise measurement of the strength of isospin forbidden gamma transitions, namely E1 decays in N=Z nuclei [13].

Shell stability and shell evolutions

Magic numbers of nucleons are fundamental quantities in nuclear structure. They have been determined on the basis of experimental information on nuclei in or near the valley of β-stability. Recently, in connection with the development of radioactive beam facilities, the question has been raised if the same magic numbers persist far from the stability line. $^{100}_{50}Sn_{50}$ is the heaviest particle-bound doubly-magic nucleus with equal number of protons and neutrons. This system and the nuclei in its vicinity provide a unique opportunity to study the interaction of protons and neutrons in a many-body system [14]. Along the Z=50 isotopes the evolution of nuclear properties as the neutron number increases is of extremely high interest, especially when approaching the other limit, the neutron drip line, close to ^{150}Sn, after which nuclei are no longer bound. A related topic is the spin-orbit splitting of the mean-field orbitals and its dependence on a more diffuse nuclear surface. If it changes for neutron rich nuclei, this could strongly influence the magic numbers for nuclei far from the stability line. Radioactive ion beams will therefore play a very important role in investigating nuclear properties far from stability. Spectroscopic studies of neutron-rich nuclei not very far from the stability line can at the moment also be performed through deep inelastic reactions, where several nucleons are interchanged between projectile and target. Information has been obtained with EUROBALL by using γ-ray coincidences between the two partners (target- and projectile-like) for the identification of unknown γ-decays.

Future perspectives with gamma detector arrays

Present gamma detector arrays are already very sophisticated instruments able to search for very weak reaction channels. New perspectives in the field of nuclear structure will be opened both by the use of high intensity beams of stable ions combined with an increasing selectivity of the instrument, as well as by the availability of moderately intense beams of radioactive ions. The combined use of γ-ray detector arrays and of magnetic spectrometers for reaction channel selection has been successfully exploited in the past and will be further developed at Jyväskylä in Finland and at LNL where EUROBALL detectors will be used to study the level structure of exotic nuclei identified respectively by the RITU gas filled separator and by the PRISMA magnetic spectrometer.

Nuclear Structure perspectives using high intensity beams of stable ions

High intensity beams of stable ions offer an interesting possibility to extend our knowledge of nuclear structure both for proton-rich and moderately neutron-rich nuclei. Quasi-elastic or multi-nucleon transfer reactions can be used to populate moderate neutron-rich nuclei along shell closures where nuclear structure calculations predict radical changes in the shell structure. Particularly powerful is the combination of large-acceptance high-resolution magnetic spectrometers with highly segmented Ge detector arrays. An high granularity of the γ-ray detector array provides for a good γ-energy resolution allowing a proper treatment of the Doppler effect. A system combining the new magnetic spectrometer (PRISMA) with the composite Ge detectors (Clovers) of EUROBALL is now coming into operation at LNL in Italy using the high intensity stable ion beams of the accelerator complex (PIAVE-ALPI).

Radioactive ion beams and gamma spectroscopy

The use of beams of unstable ions will finally allow nuclear structure studies for the most exotic systems. We should mention here the future EUROBALL detector campaign at GSI (Germany), the Rising project. Gamma-ray spectroscopy of nuclei from exotic beams will be performed after in-flight isotope separation. The exotic beams will be produced by fragmentation of heavy stable primary beams or by fission of a ^{238}U beam on a ^{9}Be or ^{208}Pb target and then selected by the fragment separator. Other γ-ray detector arrays are now starting operation at radioactive ion beam facilities such as Spiral (Ganil, France) or Rex-isolde (CERN, Switzerland).

Increasing the sensitivity of germanium-detector arrays by γ-ray tracking

Gamma-ray detector arrays of the present generation are built of Compton-suppressed Ge-detectors arranged in tightly packed spherical configurations. High granularity (and large distances from the target position) is needed for an efficient Doppler shift correction.

This is achieved by rejecting the signal from the detector when the surrounding BGO scintillator shield detects γ-rays that are Compton scattered out of the Ge crystal. It is now the common

view that in order to make the next major advance, the suppression shields have to be replaced by active Ge detectors. The major problem here is the uncontrollable Compton scattering. A solution is that all γ-ray interaction paths need to be tracked and characterized—see figure 8.

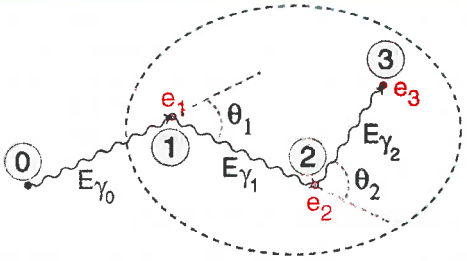

▲ **Fig. 8:** A Compton scattering event inside a Ge detector having three interaction points. Tracking of the gamma ray can be achieved through precise measurements of energy deposit and position at each interaction point. Digital electronics and pulse shape analysis are therefore essential. The tracking reconstruction efficiency, and therefore the total efficiency of the system, will be strongly dependent on the position resolution, which can be brought to few millimeters.

The recent advances in crystal segmentation technology and digital signal processing have opened the possibility to operate the detectors in a position-sensitive mode with high counting rates. This enables the design of a compact array solely out of Ge detectors omitting the BGO shields (Advanced GAmma ray Tracking Array). It is expected from simulations that an array consisting of a limited number (~ 50 - 100) of such detectors can have unprecedented features: an efficiency of up to ~ 40% while maintaining a signal over noise-ratio of the order of 60%. Therefore by using the tracking technique one expects to improve the array sensitivity by about two orders of magnitude over the current generation of Ge-arrays. A wide European collaboration is now progressing in this way [15].

References

[1] Boynton *et al.*, *Science* 297 (5578):81 R24 and http://grs.lpl.arizona.edu

[2] J.Simpson, *Z. Phys* A358 (1997)139

[3] NewScientist, 8 June 2002, page 7 and J. Dudek *et al. Phys. Rev. Lett.* 88 (2002) 252502

[4] G. Benzoni *et al.*, *Phys. Lett.* B 540 (2002) 199

[5] S. Toermaenen *et al.*, *Phys. Lett.* B 454 (1999) 8

[6] S.W. Ødegård *et al.*, *Phys. Rev. Lett.* 86 (2001) 5866

[7] D.R. Jensen *et al.*, *Phys. Rev. Lett.* 89 (2002) 142503

[8] W. von Oertzen, *Eur. Phys.* J. A11 (2001) 403

[9] G. Baldsiefen *et al.*, *Nucl. Phys.* A 574 (1994) 521

[10] R.M. Lieder *et al.*, *Eur. Phys.* J. A13 (2002) 297

[11] S. Frauendorf, *Nucl. Phys.* A 557 (1993) 259c

[12] S. Lenzi *et al.*, *Phys. Rev. Lett.* 87 (2001) 12250

[13] E. Farnea *et al.*, *Phys. Lett.* B (2002)

[14] C. Fahlander *et al.*, *Phys. Rev.* C 63 (2001) 021307(R)

[15] R. Lieder *et al.*, *Nucl. Phys.* A682(2001)279c

Teaching mathematics to physicists in the UK – *FLAP* and PPLATO

M.H. Tinker, J.J. Thomson Physical Laboratory, Whiteknights, University of Reading, UK

In the late 1980s a problem began to emerge in the UK with mathematics teaching for undergraduate physics. A broader 16-19 curriculum in schools had encouraged more flexible study patterns, threatening the traditional pairing of A-Level physics and A-Level mathematics. Increasingly, students were studying physics without mathematics and although these students were not usually intending physics degrees the syllabuses for physics and mathematics began to evolve separately. Physics was taught with less mathematics and mathematics was taught with less reference to physics. This decoupling of the two subjects produced an undergraduate physics intake that was less comfortable with using mathematics in physics, even those with good grades in both subjects. Physics departments had to restore the relationship between physics and mathematics expected of a professional physicist. The problem was exacerbated by the common practice in universities of having service mathematics taught to physicists by mathematics departments. This tended to continue the decoupling rather than to restore the link. The realisation that mathematics, like other skills needed by a physicist, had to be securely embedded within the main subject teaching began to gain favour in the early 1990s. The changing patterns of A-level study also encouraged more flexible entry routes into physics degree courses for those without traditional A-level backgrounds in physics and mathematics. This led to the introduction of Foundation or Access year programmes as a precursor to three year BSc Physics programmes.

In 1992, following an initiative by the Institute of Physics in 1989, the project *FLAP* (Flexible Learning Approach to Physics) began [1]. *FLAP* was led by the University of Reading and the Open University as a consortium project on behalf of the university sector. Over 5 years it received £780K of funding from the UK Higher Education Funding Councils. It produced a high quality supported self-study resource covering first year and foundation year physics and its associated mathematics. This generous support allowed the production of extensive new text materials, designed for the purpose and unlike any pre-existing textbooks in physics or mathematics. It was described by some as a "breath of fresh air". It allowed physics departments to create courses to their own design and specification in response to a diversifying and changing intake. Key features were its linking of physics and mathematics and its flexibility. It was first delivered in 1995.

◀ **Photo:** Teaching with *FLAP* and *Hyperflap*.

Although *FLAP* was a response to a UK university problem, its flexibility and the global nature of the problem addressed extended its impact to schools and internationally. The resource and its evaluation have been described in detail elsewhere [2]. The factors that gave birth to *FLAP* still exist today and its approach remains relevent. In this article we give a brief description of the resource and its approach. We then describe how, in 2003, it is being incorporated into a new suite of digital resources under the banner of a newly funded project PPLATO – Promoting Physics Learning And Teaching Opportunities.

The Flexible Learning Approach to Physics

FLAP consists of text, audio, video and computer materials. The text consists of 83 free-standing modules in two parallel strands of physics and mathematics (See Appendix). Module titles show the scope of the resource. In mathematics, the range is from simple algebra (e.g. the expansion of brackets in Module M1.1) to the time-dependent Schrödinger equation (Module M6.4). In physics, the range is from the definition of SI units (Module P1.1) and linear motion (Module P2.1) to the angular momentum eigenstates of atomic hydrogen (Module P11.3). This range covers the physics and mathematics needed in the first year of a UK physics degree course and in a year's full-time study prior to this. The mathematics strand has also been published by John Wiley as two mathematics textbooks [3-4]. The text element of *FLAP* has much in common with textbooks in that it can be used to support lectures, tutorials, workshops and laboratory teaching, but there are several important differences from a conventional textbook:

- It has a completely new modular text, written specifically to cope with diversity and to reinforce the relationship between physics and its associated mathematics.
- It uses a common approach to physics and mathematics, presenting mathematics thoroughly, yet within a physical context where possible and with due regard to dimensions and units.
- It is more flexible in use, both for students and course designers. Each free-standing module specifies pre-requisite knowledge, measures student background via formative tests and provides differentiated study routes accordingly. This means that modules have no fixed order of study, quite unlike the chapters of a standard textbook, and study patterns are set by course designers and are automatically customised to the individual student.
- Its scope and depth is more extensive—its size is equivalent to about five major textbooks, two in mathematics and three in physics, but the modular structure maintains portability.
- It is sufficiently detailed to form a primary teaching vehicle, so it may be used in self-study or to replace some teaching contact time, allowing more individual and targeted support.
- It may be photocopied by an institution for its own students, allowing customised textbooks to be produced at a fraction of the cost of a normal textbook. Students do not have to purchase unwanted material or the latest edition of standard texts. The only penalty paid for being photocopiable is the removal of colour in the printed material.
- It trains students to become independent learners by using supported self-study to engage them in active learning and by encouraging reading and time management skills.
- It develops the students' knowledge and skills base, adopting a problem-solving approach with embedded questions designed to develop cognitive skills, raise conceptual understanding and challenge pre-conceptions.

- It gives the student more ownership and control of the learning through the differentiated routes through the material.

The scale of the *FLAP* resource is best illustrated by its full contents as summarized below. It contains material equivalent to about 200 lecture hours or 500 study hours and includes:

- 83 *FLAP* modules as single-sided A4 monochrome photocopy card masters (about 2250 pp).
- 1 *Index*, *Student Guide* and *Maths Handbook* (also as photocopy masters).
- Photocopying license for an institution to use to make copies for its own students.
- 1 ring bound browsing copy of all 83 *FLAP* modules.
- 1 ring bound copy of the *Glossary* (about 2500 entries), *Scientific Biographies*, *Maths Handbook* and *Index*. The *Glossary* is a relational glossary, combining the functions of index, dictionary and thesaurus, not only listing definitions but also showing how they relate to one another across the full range of the package. The *Glossary* is also the main routing document in *FLAP*. Modules contain no explicit reference to other modules and all such links are made through the *Glossary*. This feature maintains module independence and maximises flexibility.
- *Tutor Guide Part 1*, including product description, module outlines and guidance on use.
- *Tutor Guide Part 2*, is a question bank of about 1700 extra questions with fully worked answers. Questions and solutions are on computer disk, allowing convenient cutting and pasting for assessment production.
- A *Hyper-glossary* and *Index* on disk (about 2500 entries and 15000 hyper-links). This is an HTML document with about 3000 embedded graphic links and 15000 intra-glossary links. It includes an index of terms and biographies of many of the scientists and mathematicians who have contributed most to the development of the field.
- A *CAL package* on disk, including interactive simulations on *Electric fields*, *Bubble chamber*, *Gas simulation*, *Orbital motion*, and a *Forces tutorial*.
- A *CAT-FLAP package* on disk. This computer-administered self-assessment diagnostic tool contains over 400 multiple choice questions and solutions from all the modules. It also contains three diagnostic access tests, two for physics and one for mathematics. A printed report can be generated for tutor discussion and tutors may add their own questions and solutions.
- 8 C60 audio-cassette tapes, including interactive tutorials
- 4 E30 video tapes, including animations and demonstrations

Module structure

The internal structure of the modules is one of the most powerful innovations of *FLAP*. It is this that allows flexible, differentiated access for students. Students measure their backgrounds for the topics to be introduced and can plan their study time most efficiently. They may move speedily over familiar ground, reviewing it as necessary, but spend more time building new knowledge and skills. The text has a programmed approach, with interactive decisions controlling the route, as shown in the flow chart in Figure 1.

Each module begins with a diagnostic section entitled *Opening items*, which sets the scene, introduces the topics and invites students to assess their background knowledge. The material may be mostly old knowledge, mostly new knowledge or a reasonable extension of old knowledge. There are *Fast track* questions to test whether it is old knowledge and *Ready to study* questions to test whether more preparation is needed. Solutions are given for all these questions to guide students in their choice of route. The *Fast track* route leads quickly to the *Exit test* at the end of the module, where the wisdom of this choice of route can be self-tested. Students who need help with the *Ready to study* questions are directed through the *Glossary* to other *FLAP* modules. Students who determine that they are ready for the material move on to the main teaching text of the module. Field trials show that students quickly develop the skills to use this diagnostic front-end and to make best use of their study time.

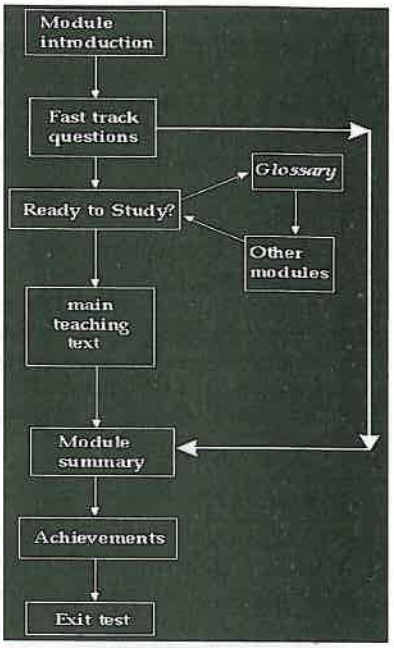

▲ **Fig. 1:** The structure of a *FLAP* module.

The main teaching text of each module is written in a clear, student friendly, interactive style, laced with short in-text questions and longer self-assessment questions to test and reinforce the learning. Students are encouraged to tackle these questions as they come to them in the text and the solutions often contain teaching comments which are essential for subsequent parts of the main text. Important terms are highlighted and flagged in the margins, major equations are boxed and asides or explanations of details are given in marginal notes. Questions are often of the type which confront pre-conceptions and encourage conceptual thinking.

After the main text there is a section entitled *Closing items*. This contains a detailed but concise *Module summary*, followed by a list of the *Achievements*, or learning outcomes for the module. These are written in operational terms, explain what students should be able to *do*, and identify what is required for assessment purposes. The *Closing items* concludes with an *Exit test* to test the learning outcomes. All routes pass through the *Closing items* since it provides valuable feedback and revision. Detailed solutions to all questions are at the end of the module, so students can assess their own progress. Evaluation has shown that an average module is equivalent in content to about 2 or 3 lecture hours and requires 5 to 6 study hours by the standard route.

Using *FLAP*

FLAP is a very large resource, not a course, and how it is used is determined by the individual teacher. The flexible structure allows *FLAP* to be incorporated easily within existing teaching programmes or to be used to design new teaching. In deciding whether to use *FLAP* the important decision is to assess the extent to which the teacher wishes to encourage independent learning, to give students more control over the learning and to see the purpose of teaching as the support of learning. A likely consequence of using *FLAP* is that the teacher lectures less and discusses more. The student listens less but reads and discusses more. For both parties this creates more active engagement with each other and with the learning process. This approach is generally welcomed by both parties, but not universally so. Students and

teachers can be beguiled by the apparent efficiency of the lecture as a learning tool. Experience suggests it is highly optimistic to equate speaking and hearing with learning. Effective learning is active and effective teaching must accommodate a variety of learning styles [5-7]. Within this general picture *FLAP* has been used successfully in many situations, such as those below.

- Pre-course work for entry to a degree programme (taught or self-study)
- Diagnostic testing on entry to a degree programme or within such a programme
- Consolidation of background on entry to a programme
- Support for main-stream lecture courses
- Replacement of a conventional lecture course by a *FLAP*-based course having fewer lectures
- Creation of a complete supported self-study programme (e.g. as a Foundation Year)

Evaluation

FLAP has been evaluated extensively since it was first used at the University of Reading in developmental testing in 1993. Overall comments from all these evaluations is that when used as part of a teaching programme *FLAP* brings benefits to the student, the teacher and the institution.

Staff point to benefits from improved student effort, study discipline, organisational skills and motivation and in the teacher's ability to deal with class diversity through more focussed contact time. There are the benefits from embedding mathematics within the physics. The extensive question bank significantly reduces staff effort for testing and diagnostics. Teaching assistants make a more effective contribution through access to the same teaching materials as the students.

Students are generally enthusiastic about the *FLAP* learning style, recognize the benefits of active learning and welcome their increased ownership of the learning. They respond with increased motivation, commitment and success. They gain more self-confidence, interact better with each other and with staff and feel more confident about their learning and understanding. Reading skills are improved and students find the 'fast track' route through the modules is an excellent revision tool. Overall, students welcome *FLAP* self-study, in conjunction with some lectures, workshops or tutorials. However, active learning is not universally appreciated. A minority of students prefer to remain passive, since it places fewer demands on them. Initially, this group may be quite vocal and the general view may take a while to emerge from the noise.

e-FLAP

From 1996 the *FLAP* project has been ongoing as a self-funding operation. Five new modules, covering relativity, particle physics, vector calculus, matrices and determinants are about to be released. An electronic copy of the original modules, *e-FLAP*, has been produced on CD ROM. This may be licensed either for single users, or for institutional use on up to 10 machines or on a local area network. *e-FLAP* allows users to have quick reference to any part of the text resource or to produce their own printed copies of the modules or parts of the modules.

Hyperflap

Hyperflap is a further development in progress. This contains the full *e-FLAP* text but is designed for screen use and has hyper-links within modules, between each module and the *Hyperglossary* and thereby to other modules. *Hyperflap* has several innovative features to enhance its use in teaching and learning. The text is broken down into small segments that are viewed without scrolling. Each segment also includes all required equations, figures or tables to which it refers. All hyper-links have been selected by hand on educational grounds, not generated automatically by software. *Hyperflap* will eventually become a multimedia resource, with audio, video and simulations embedded. The scale and nature of the resource will make it unique.

The project is prepared to release developmental evaluation copies of *Hyperflap* to a limited number of institutions in conjunction with their use of *e-FLAP* or the paper version of *FLAP*. Interested institutions should contact the author.

PPLATO PROMOTING PHYSICS LEARNING & TEACHING OPPORTUNITIES

Promoting Physics Learning And Teaching Opportunities — PPLATO

In November 2002 *FLAP* and *Hyperflap* became part of a larger project, PPLATO, again funded through the Funding Councils. This is a Consortium project led by the University of Reading with Brunel University, the Open University, the University of Newcastle, the University of Plymouth and the University of Salford. It addresses the twin problems of teaching mathematics to physics undergraduates and widening participation in undergraduate physics. It will produce flexible resources for face-to-face or on-line delivery and for use within an institution in an accredited programme or for self-study. A particular remit is to develop a Foundation Programme suitable for physicists and engineers. It will survey current practice in the sector and build on previous successful developments and experiences. Project outcomes are expected to be improved student competence in mathematics and physics and wider participation and improved retention in undergraduate physics. New resources will include flexible materials for teaching, diagnostics, assessment and tutorial support, with effective strategies for their use. Institutions wishing to take part in this undertaking and to have access to the developing resources should contact the author.

References

[1] Lambourne, R.J.A., and Tinker, M.H.; The Flexible Learning Approach to Physics: *FLAP*; *Physics Education*, **28** 1993, 311-316

[2] Tinker, M.H., Lambourne, R.J.A., and Windsor, S.A.; The Flexible Learning Approach to Physics (*FLAP*) - a review after the first two years; Int. J. Sci. Educ. **21**, 2, Feb 1999, 213-230 Taylor & Francis

[3] Robert Lambourne and Michael Tinker; Basic Mathematics for the Physical Sciences;
John Wiley & Sons, Ltd./OU, February 2000, 674 pp

[4] Michael Tinker and Robert Lambourne; Further Mathematics for the Physical Sciences; John Wiley & Sons, Ltd./OU, April 2000, 730 pp

[5] McDermott, L.C.; Millikan Lecture 1990: What we teach and what is learned - Closing the gap; *Am. J. Phys.*, **59**, 1991, 301-315

[6] Redish, E.F.; Implications of Cognitive Studies for teaching physics; *Am. J. Phys.*, **62**(9), 1994, 796-803

[7] Van Heuvelen, A.; Learning to think like a physicist: A review of research-based instructional strategies; *Am. J. Phys.*, **59**, 1991, 891-897

Appendix

FLAP physics modules

P1 Measurement
P1.1 Introducing measurement
P1.2 Errors and uncertainty
P1.3 Graphs and measurements

P2 Mechanics
P2.1 Introducing motion
P2.2 Projectile motion
P2.3 Forces
P2.4 Work and energy
P2.5 Momentum and collisions
P2.6 Circular motion
P2.7 Rotational mechanics
P2.8 Angular momentum

P3 Fields
P3.1 Introducing fields
P3.2 Gravitation and orbits
P3.3 Electric charge, field and potential

P4 Electricity and magnetism
P4.1 DC circuits and currents
P4.2 Introducing magnetism
P4.3 Electromagnetic force
P4.4 Electromagnetic induction.
P4.5 Energy in electric and magnetic fields

P5 Vibrations and waves
P5.1 Simple harmonic motion
P5.2 Energy, damping and resonance
P5.3 Forced vibrations and resonance
P5.4 AC circuits and electrical oscillations
P5.5 The mathematics of oscillations
P5.6 Introducing waves
P5.7 Sound - a wave phenomenon

P6 Light and optics
P6.1 Light - a wave phenomenon
P6.2 Rays and geometrical optics
P6.3 Optical elements
P6.4 Optical instruments

P7 Heat and properties of matter
P7.1 The atomic basis of matter
P7.2 Temperature, pressure and the ideal gas law
P7.3 Internal energy heat and energy transfer
P7.4 Specific heat, latent heat and entropy
P7.5 Kinetic theory - an example of microscopic modelling
P7.6 Mechanical properties of matter

P8 Atoms and molecules
P8.1 Introducing atoms
P8.2 Atomic spectra and hydrogen
P8.3 Multi-electron atoms
P8.4 Periodic Table and chemical bonding

P9 Nuclei, particles and relativity
P9.1 Introducing atomic nuclei
P9.2 Radioactive decay
P9.3 Fission, fusion and radiation hazards

P10 Principles of quantum physics
P10.1 A particle model for light
P10.2 A wave model for matter
P10.3 Wave functions
P10.4 The Schrödinger equation

P11 Applications of quantum physics
P11.1 Reflection and transmission at steps and barriers
P11.2 The quantum harmonic oscillator
P11.3 Schrödinger's model of hydrogen
P11.4 Quantum physics of solids

FLAP mathematics modules

M1 Algebra, functions and equations
M1.1 Arithmetic and algebra
M1.2 Numbers, units and physical quantities
M1.3 Functions and graphs
M1.4 Solving equations
M1.5 Exponential and logarithmic functions
M1.6 Trigonometric functions
M1.7 Series expansions and approximations

M2 Vectors and geometry
M2.1 Introducing geometry
M2.2 Introducing co-ordinate geometry
M2.3 Conic sections
M2.4 Introducing scalars and vectors
M2.5 Working with vectors
M2.6 The scalar product of vectors
M2.7 The vector product of vectors

M3 Complex numbers
M3.1 Introducing complex numbers
M3.2 Polar representation of complex numbers
M3.3 Complex algebra and de Moivre's theorem

M4 Differentiation
M4.1 Introducing differentiation
M4.2 Basic differentiation
M4.3 Further differentiation
M4.4 Stationary points and graphing
M4.5 Taylor expansions & polynomial approximations
M4.6 Hyperbolic functions and differentiation

M5 Integration
M5.1 Introducing integration
M5.2 Basic integration
M5.3 Techniques of integration
M5.4 Applications of integration
M5.5 Further integration

M6 Differential equations
M6.1 Introducing differential equations
M6.2 Solving first order differential equations
M6.3 Solving second order differential equations
M6.4 Waves and partial differential equations

About the author

Mike Tinker is a Senior Lecturer in Physics at the University of Reading. His research interests are biophysics and physics education. In physics education Mike was one of the two central academics involved in the development of the Flexible Learning Approach to Physics (*FLAP*) resource for the UK Higher Education sector. He is a Fellow of the Institute of Physics and in 2002 was the joint winner of their Bragg Medal and Prize for Physics Education. In 2002 he was awarded £250K from the Higher Education Funding Councils to lead a consortium project PPLATO (Promoting Physics Learning and Teaching Opportunities). He is married with two children, both now fully free in an unsuspecting world.

Quantum optics with gamma radiation

Romain Coussement[1,2], Rustem Shahkmouratov[1,3], Gerda Neyens[1] and Jos Odeurs[1]
[1]Instituut voor Kern- en Stralingsfysica, Katholieke Universiteit Leuven, Celestijnenlaan 200 D, B-3001 Leuven, Belgium
[2] Optique Nonlinéaire Théorique, Université Libre de Bruxelles, CP 231, Bld du Triomphe, B-1050 Bruxelles, Belgium
[3]Kazan Physico-Technical Institute of Russian Academy of Sciences, 10/7 Sibirsky trakt, Kazan 420029, Russia

CAN one slow down a gamma photon to a group velocity of a few m/s, or can one stop it in a piece of material only a few micron thick and release it? Can one, on command, induce transparency of a nuclear resonant absorber for gamma radiation and make a gate? Can one change the index of refraction for gamma rays in such a way that one could think of optical devices for gamma radiation such as mirrors, cavities etc?

Such questions would all sound like science fiction if we did not know that such effects were first predicted by theoretical quantum optics and are observed experimentally with optical photons interacting with atoms [1-4]. Since gamma radiation and optical radiation are of the same electromagnetic nature, we can ask seriously why we could not observe the same effects when gamma radiation interacts with nuclear matter. These are the questions that one tries to answer in the field of "quantum nucleonics", sometimes also called "gamma optics".

There are obviously some important differences between quantum optics (interaction of photons with atomic electrons) and gamma optics (interaction of gamma photons with atomic nuclei). In particular for the investigation of the former the basic ingredient is the use of laser light (called the 'driving' laser) for inducing coherence and interference effects in atomic systems with three or more levels (Box 1: the basic principles of coherence and interference).

The exploration of coherence with gamma radiation has been hindered by the fact that one does not have a driving gamma ray laser. Furthermore, gamma radiation is emitted by a radioactive source and there is no phase coherence between photons as is the case for photons emitted by a laser in the optical domain. But this restriction can be circumvented to a large extent by the use of mixed level doublets in the nucleus (Box 2). We will show that the study of coherence and interference with gamma radiation has some unique features compared with the optical case.

First one should note that the gamma photons are emitted and detected as single photons. This is a restriction, but it also provides a unique opportunity to see interference effects using a single photon. Optical single photon experiments require sophisticated equipment (which is available but needs special care and skills), while with gamma radiation each experiment is a single photon experiment. It allows us to address some fundamental questions about the quantum mechanical, dual nature of the single photon.

Another interesting feature is that one can easily choose gamma rays emitted from a nuclear isomer. Because of the long lifetime of the isomeric state, its line width is extremely small and the coherence length of the emitted photon is very long. For the gamma rays of 14.4 keV emitted by the excited ^{57m}Fe state (τ= 141 *ns*, I=3/2), the coherence length is about 40 m. For the 6.2 keV gamma radiation from ^{181m}Ta, having a lifetime of 8.73 μs, the coherence length is 4 km. The appreciable coherence length of these gamma photons allows us to observe the interference between the transition amplitudes from two paths of the single photon, passing through two different samples. In one path the photon interacts with nuclei of a reference sample and in the other path it interacts with the nuclei of a sample under investigation. The distance between the samples can be as large as the coherence length of the photon. Interference of these two transition amplitudes provides spectroscopic information about the hyperfine interaction of the nuclei in the investigated sample, provided the hyperfine spectrum of the nuclei in the reference sample is known. Such interference phenomena have been explored using synchrotron radiation [5] and are nowadays used as a tool for solid state physics studies.

Since the discovery of optical lasers, the scientific community has been challenged to realise a gamma ray laser.

Because of their very high energy, the gamma photons have very short wavelengths: of the order of an Angström or a fraction of it. Consequently, it becomes possible to investigate crystalline structures using nuclear Bragg scattering. Methods based on this feature, such as nuclear emission [6] and absorption holography [7], have been explored recently.

Having photons with a very long coherence length and a very small wavelength allows us to conceive an interferometer that is very sensitive to small changes in optical length. The idea has not yet been explored and one of the possible applications may be the detection of the gravity red shift with a much higher precision [8].

Because nuclear cross sections are many orders-of-magnitude smaller than the atomic ones, nuclear gamma optics experiments require the use of high density targets, which means the use of

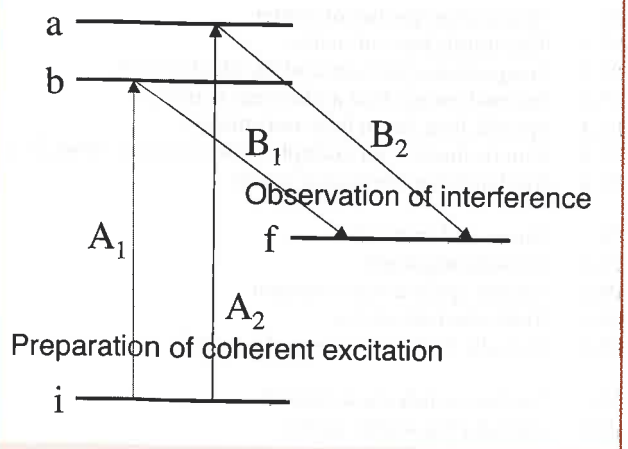

▲ **Fig. 1:** The levels *a* and *b* can be coherently excited by the fields A_1 and A_2 provided that both fields are locked in phase. In a subsequent process, in which these states make a transition to the same final level, interference can be observed.

solid materials. As the nuclear recoil energy induced by the gamma decay is very large (because of the large gamma ray energy) and because the recoil energy depends on the spectrum of phonons created in the lattice, the gamma ray emitted from a nucleus embedded in a solid has a large statistical energy distribution. To allow experiments with narrow gamma lines it is necessary to use solids in which this large statistical energy variation is reduced. This is a major restriction on the gamma transitions available for gamma optics research, as only Mössbauer isotopes fulfill this condition. For such isotopes the recoil momentum is transferred to the lattice as a whole and the gamma decay is registered as a 'recoilless' decay, giving rise to narrow gamma ray lines. One could lift this restriction by using dilute gases or mono-energetic beams of nuclear isomers [9]. The recoil energies would then be the same for all events, and averaging all transition amplitudes over a large ensemble of events would not lead to the cancellation of the interference term. However the smallness of the densities together with the small cross sections put such experiments out of reach with the present means of producing nuclear isomers.

The gamma ray laser

Since the discovery of optical lasers, the scientific community has been interested and challenged to realise a gamma ray laser (see for example [12]). A gamma ray laser would offer many applications because of the short wavelength and because of the high power density. Despite the considerable efforts of many groups, there still exists no idea of how to build such a device using present technology and our available knowledge of laser, nuclear and atomic physics.

The main problem is the realisation of population inversion. Because of the small cross sections for nuclear photo-absorption, an adequate pump mechanism does not exist. Because the pump efficiency is very weak, while the losses due to electronic absorption processes are important, one needs a tremendous energy input. Under extreme pump irradiation, the non-resonant power input would be so large that the sample would be destroyed by melting or evaporation before lasing could occur. As a result we are faced by the so called gamma laser dilemma [13] in that one needs a solid with a high recoilless fraction and that the condition for recoilless fraction will be destroyed by the required pump power. To try to circumvent this dilemma, one follows two avenues. They have in common that one will store energy in long-lived isomers and find a mechanism to release it on command. Storing large amounts of energy in nuclear isomers is not the real challenge. One can produce these long-lived isomers in nuclear reactors or with accelerator beams and separate them from other types of material by chemical and/or physical means. The technology is available in principle or at least there is enough knowledge available for it to be developed. The problem is the release of the stored energy 'on command' and in a very short time. It is on this point that the two approaches diverge conceptually.

Energy conversion

One of the roads followed is to pump a long-lived nuclear isomer into an excited nuclear state via low energy X-ray irradiation. Subsequently this excited state decays via the emission of gamma rays, representing a multiple of the input energy (see figure 3). In this scenario the long-lived isomeric state could act as a nuclear battery, in which energy is stored.

A proof of principle for releasing the stored energy has been demonstrated using a K-isomer as the storage level [14]. From the point of view of nuclear models the result is surprising. Indeed,

features

Box 1

Coherence and Interference

A quantum transition from state i to state f can be described by an amplitude $A = A'_{if}\exp(i\varphi)$, where φ stands for the phase of the field inducing this transition and A'_{if} is the complex transition matrix element, which depends on the relative phases of the initial and final states. In most processes all the phases are cancelled since the observable is just a transition probability $P = |A|^2$. However, if the experiment is designed in order to observe a process with two quantum paths, one must first sum the amplitudes and then square the norm. This procedure will produce interference terms in which the phase factors play an important role:

$$P = |A_1 + A_2|^2 = |A_1|^2 + |A_2|^2 + [A'_1A'^*_2e^{i(\varphi_1-\varphi_2)} + A'^*_1A'_2e^{-i(\varphi_1-\varphi_2)}] \quad (1)$$

In an experiment a large number of events is observed. If all the phases are different from event to event then the experimentally observable is an average of all possible phase differences. The interference term cancels and the probability is just the sum of the partial probabilities $P_i = |A_i|^2$.

However one can design an experiment in which the interference term is not zero. Then the interference is constructive or destructive, depending on the sign of the phase difference $\varphi_1-\varphi_2$, if the latter is fixed for the ensemble or chain of events. This can be done if the transition is split in two paths due to the two-step processes, as shown in Fig. 1. In one step (A_1 and A_2) the coherence between a and b states is prepared, if the phase difference of the A_1 and A_2 fields is fixed (which is the case of the phase locked fields or mutually correlated fields). In the second step (B_1 and B_2) the interference is observed. The arbitrary phase of the intermediate state does not affect the result because this state occurs with its complex conjugate in the transition amplitude from state i to state f, i.e., $(A'_1)_{ib}(B'_1)_{bf}$. When calculating the transition probability of two quantum paths, each following a two-step process (Fig. 1), the phase factors of the initial and the final states cancel, provided that both paths start and end at the same initial and final states. Coherent preparation is mostly called coherent excitation and the interferences are observed in the subsequent step. However the role of the preparation and observation step may be reversed. In that case the interferences can be observed in the first step, provided that the experiment is constructed such that the observed transition in the first step is conditioned by the second step.

In short, the rule for observing interference in quantum transitions is that the observed transition can pass via two indistinguishable quantum paths, which have a common initial and a common final state, and that the radiation fields in the preparation step are phase locked.

While in quantum optics the phase locking of the laser fields became a routine, in case of gamma radiation, where single photon processes are to be considered, this problem needs special care. To be coherent the first step of excitation must go to closely spaced nuclear levels. These levels are to be close enough in energy that a single photon can induce the transition to the two states, despite its sharp frequency distribution. In box 2 we explain how to produce such closely-spaced nuclear levels and later in this article we demonstrate that they fulfill all the conditions to be coherently excited by a single gamma photon.

the K-isomeric state has a long lifetime because the K-selection rule hinders its decay into nuclear states at lower energy as this involves a large change in the projection of the angular momentum [15]. It comes as a surprise that the transitions to higher energy states in this ground state band are then less affected by this hindrance. It is certainly an interesting phenomenon for nuclear spectroscopists. However because of the weak coupling of the X-ray pump with the possible lasing level, this is not yet an efficient mechanism for producing a gamma ray laser.

Lasing without inversion

A prime condition for gain with stimulated emission is population inversion, or explicitly, the number of excited state nuclei from which lasing has to occur, exceeds the number of ground state nuclei. This condition requires that one must be able to perform a nuclear isomeric separation in order to obtain nearly pure isomeric material. Such a technology could be developed in the future, for example using the laser ionisation method for producing isomeric enrichment, the separation being based on the difference in the hyperfine structure [16].

Even if a solid material could be prepared with most of the nuclei in the ground state as well as a large number in some long-lived isomeric state, without having an inverted system, lasing might still be realised. To obtain lasing from such a system, the concept of "lasing without inversion" as introduced in quantum optics, could be translated to gamma radiation. In the optical range the effect of "lasing without inversion" has been demonstrated experimentally [4] and it was pointed out that the main new application will be the realization of lasers at very high frequency, for example UV, X-ray or even a gamma ray laser. The main point here is that one can create coherence in a three level system in such a way that absorption of the lasing frequency is cancelled by destructive interference while the emission, and in particular the stimulated emission, is not [18].

In optics one can coherently excite two atomic levels by irradiating the atoms with two lasers of different frequency (color) but coupled in phase. Such phase-locked, two-frequency laser light is called 'bichromatic light' and can easily be obtained from one laser using frequency doubling or dividing crystals.

One does not have an equivalent tool in gamma optics. Therefore one is restricted to excitations of two 'nuclear hyperfine levels' which can be excited with a single gamma photon despite its small natural line width. Two conditions need to be fulfilled for this. One, the energy difference between these two levels must be less than the natural line width of the photon. This condition can easily be fulfilled by the method of nuclear level mixing, also sometimes called nuclear level anticrossing (see box 2). Secondly, the selection rules, which apply to transitions between nuclear hyperfine levels, need to be allowed in both paths. This condition is automatically fulfilled by the nature of the mixed levels produced via nuclear level mixing: the doublet consists of an in-phase and an anti-phase superposition of m-quantum states. The selection rules, also taking into account the polarization of the photon, allow for example the transition to the angular momentum component m (which occurs in both mixed levels). Excitation of both levels of the doublet can then be achieved with a single photon.

In order to observe interference effects in this absorption process, another condition needs to be fulfilled, namely the two interfering quantum paths need to be fully coherent (see box 1). The coherence is created by the connection of the two states of the doublet with a single fourth quantum state with some resonant or quasi-resonant radiation (called the driving field). Such radiation can for example be induced by a radio frequency (rf) magnetic field (also called a Nuclear Magnetic Resonance, NMR, field) [18]. In that case the fourth level must be a member of the same hyperfine manifold. It can also be induced by the coupling between the atomic and nuclear spins, via the excitation of the atomic state. In that case the radiation can be optical [19].

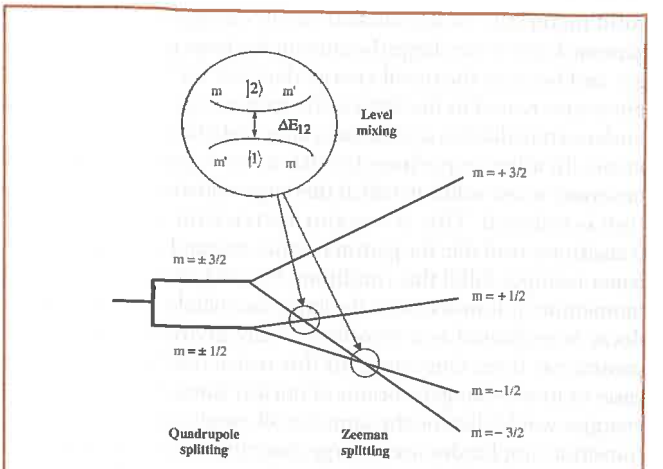

▲ **Fig. 2:** Nuclear hyperfine levels as a function of the magnetic field, for the I=3/2 isomeric state in ^{57}Fe subjected to an electric field gradient and a static magnetic field. If the symmetry axes of both interactions are parallel, crossing of hyperfine levels occurs at particular values of the magnetic field (small circles). If the axial symmetry is broken by slightly misaligning the magnetic field with respect to the electric field gradient symmetry axis, then the hyperfine levels are mixed (enlarged part around the crossing).

Another problem that remains is related to the weak coupling of the nuclei with the gamma radiation. When choosing nuclei with a very long lifetime, there is enough time to produce large quantities of the isotope, to make isomeric enrichment and to store it before triggering the release of all stored energy by turning on the driving radiation. However, there is a price to pay. As the isomeric state has a long lifetime, the coupling of the gamma radiation to the nuclei is weak. Thus the cross section for stimulated emission is small and the losses from electronic absorption can not be compensated by the gain from stimulated emission.

There could be a way out of this problem if the gamma radiation could be coupled to a collective ensemble of excited nuclei to form a state similar to a Bose Einstein condensate of atoms. In such a condensate, the probability for stimulated emission is multiplied by the number of excited nuclei in the collective ensemble. Now that Bose Einstein condensates have been produced in atomic systems, one might in the future think of ways to create a nuclear collective coherent state and thus pave the way for a gamma ray laser.

Nuclear level mixing induced transparency

Consider an ensemble of nuclei in their nuclear ground state, and that these nuclei have an excited state that is isomeric. Suppose the ensemble is submitted to the necessary conditions for creating a level mixed doublet in the isomeric state. As explained in box 1, interference in such a system can occur in the decay from such coherently excited, level mixed states, provided decay to a particular final state is observed. This final state could be a particular member of the ground state manifold, even the same state from

which the mixed states were populated. Indeed in such a scheme there are two paths which start and end on the same state so that the quantum phase factors cancel. However, one must notice that once the doublet states are excited, spontaneous decay will happen not only to one but to all members of the ground state hyperfine manifold. One can demonstrate that in the case of a spontaneous decay in a 4π geometry the sum of the interference terms will cancel. In order to observe interference in the decay process, decay to a particular final state needs to be observed which means that the 4π symmetry must be broken.

For a large ensemble of nuclei, the 4π symmetry of the re-emission can be broken to some extent because of collective decay in some directions. It is well known from theories and experiments on elastic dynamical diffraction that the re-emission in the forward direction is enhanced.

The enhancement of the radiative decay in the forward direction can be understood as a collective effect. When a photon hits the sample, it hits all the resonant nuclei in their ground state. In the quantum mechanical picture of a photon being a particle, we would say that one of these nuclei may be excited with a certain probability. In the quantum mechanical picture of the photon as a wave, each resonant nucleus can be considered as a superposition of the "ground state plus a photon" and the "excited state without a photon". In this way the photon is not absorbed by one of the nuclei but by the 'collective ensemble' of nuclei. The re-emission occurs then from this collective excitation, which is called an 'exciton'. The radiative decay from such an exciton is very special because each nucleus will give an amplitude for the emitted photon. The phases at a point of the detector will depend on the difference in optical length between two quantum paths (originating from the decay of two different nuclei). In the forward direction these lengths are equal, while in a single crystal they are proportional to an integer number of wavelengths if scattering in the Bragg directions is observed. In these directions all the individual amplitudes add up coherently and consequently the emission probability is enhanced by a factor equal to the number of nuclei involved.

We can thus conclude that for a thick absorber the radiative deexcitation in the forward direction toward the initial state is favoured over the other decay modes, including the non radiative decay modes. The enhancement in the forward direction strongly depends on the thickness of the absorber. In such conditions we can expect that interferences can be observed because, in the case of a strong enhancement, the process of excitation and subsequent deexcitation is reduced to the two dominant paths. These two paths are coherent because they both start and end on the same level. These interferences can, in principle, lead to more or to less absorption. Interferences will be observed for gamma photons which can excite both levels of the hyperfine doublet. The requirement is that the bandwidth of the incoming gamma photon must be about the same as the energy splitting of the doublet states. With the technique of nuclear level mixing (box 2), the energy splitting of two nuclear hyperfine levels can be fine tuned. An experiment was performed using the Mössbauer absorption of the 14.4 keV radiation by the ^{57}Fe nuclei in a single crystal absorber of $FeCO_3$. This material has a hexagonal close packed lattice structure, thus inducing a quadrupole splitting of the

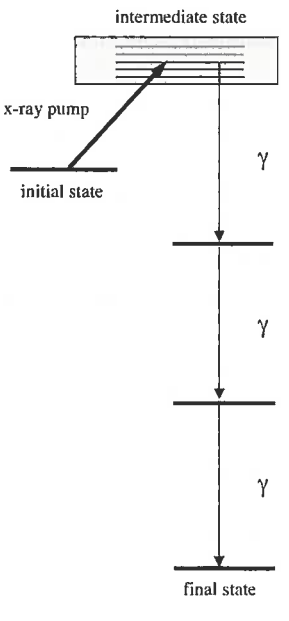

◀ **Fig. 3:** The pump scheme, using a "nuclear energy battery" as a way towards a gamma-ray laser. The initial state is a long-lived state at high spin and excitation energy (in which all nuclei are produced by some means). The state is isomeric because decay to the lower levels is forbidden by K-selection rules. The energy from this 'battery' is released by pumping it into an intermediate 'K-mixed' state, which subsequently decays via a cascade of gamma transitions. K-mixing is here the crucial ingredient to open the decay channel.

Box 2

Crossing and mixing of nuclear hyperfine levels

Consider nuclei subjected to static electromagnetic fields. The interaction of the nuclear magnetic moment with a magnetic field induces a Zeeman splitting of the nuclear m-quantum states. The interaction of the nuclear quadrupole moment with an electric field gradient gives rise to a quadrupole splitting. If both interactions are applied simultaneously and with their symmetry axis parallel, one obtains nuclear hyperfine levels as shown in figure 2. Because the quadrupole splitting is proportional to m^2, while the Zeeman splitting is proportional to m, the crossing of two quantum levels occurs at particular magnetic fields, called crossing fields, H_c. The ratio of the magnetic and quadrupole interaction frequencies determines the magnetic field at which the crossing will occur [10].

When the axial symmetry is broken slightly, because of a small misalignment of the magnetic field with respect to the symmetry axis of the electric field gradient, one can show that its effect on the quantum levels and their wave functions is negligible, except near the magnetic fields H_c where level crossing occurs. At these fields, the degeneracy of m-quantum states is lifted due to the small degree of symmetry breaking, which can be demonstrated by quasi-degenerate perturbation theory [10]. Anti-crossing of nuclear hyperfine levels occurs and the wave functions are mixed in coherent superpositions of the wave functions belonging to the crossing states. At the crossing field, the mixed wave functions form exactly an in-phase and an anti-phase superposition of m and m' (inset of figure 2):

$$|1\rangle = 1\sqrt{2}\,\{\,|m\rangle + |m'\rangle\,\} \qquad (2)$$
$$|2\rangle = 1\sqrt{2}\,\{\,|m'\rangle - |m\rangle\,\} \qquad (3)$$

The minimum energy difference between the levels occurs at the crossing field and is dependent on the strength of the symmetry breaking term, which is determined by the misalignment angle between the applied interactions. Thus we can adjust the energy difference between the two levels.

Such mixing nuclear hyperfine states have been used in several fields of physics. For example as a tool to investigate the structure of solids using synchrotron radiation [5] or as a tool to study the structure of exotic nuclear states using their anisotropic radioactive decay [11]. They may also provide a step towards a gamma ray laser, as discussed later in this article.

nuclear levels in ^{57}Fe. Below 40 K, the material becomes magnetic as well, thus allowing the fulfilment of the level mixing conditions (figure 2). In a Mössbauer absorption measurement, the intensity in the Mössbauer line corresponding to the absorption into the level mixed doublet, does not correspond to the sum of the intensities of the individual transitions [20]. This is a clear signature for the presence of interference effects in nuclear gamma ray absorption towards level mixed nuclear hyperfine levels. Moreover the effect of coherence is demonstrated for single photon events.

Slow group velocity for gamma radiation?

From classical electromagnetism it is well known that an electromagnetic pulse can propagate through a resonant medium with a group velocity that can be much slower than the phase velocity or the velocity of light [21]. The effect derives from the fact that near a resonance the index of refraction changes drastically. Therefore, each frequency component of the pulse will have another velocity, resulting in a slower propagation of the pulse shape through the medium. In a two level system it is difficult to observe the effect because, at resonance, there is strong resonant absorption and, consequently, the pulse will be just absorbed and not transmitted to the detector.

In a three level system, however, the absorption is cancelled in the energy (or frequency) region about halfway between the doublet levels. Exactly in that region, the index of refraction changes enormously [4] and consequently the group velocity can be much slower than the velocity of light. From the transparency that was observed in the Mössbauer experiment [20] one can estimate that the propagation velocity of the gamma photon is reduced to about 1 km/s.

Conclusions

Coherence and interference effects in the interaction of light with matter led to very interesting and somewhat unexpected results in the field of quantum optics, such as gain without inversion, electromagnetically induced transparency, changes in index of refraction etc. [4]. In the challenging quest for a laser with gamma radiation these phenomena have been suggested as possible solutions to the gamma-ray laser dilemma. For that, a translation of the optical phenomena into the field of gamma optics, the interaction of gamma radiation with nuclei, has to be performed. A rich field of research related to coherence and interference in gamma radiation has evolved out of this.

Because of the single photon character of nuclear events, the conditions for coherence and interference need to be realized in a very different way. For example the bichromatic driving field that is used in optics, is replaced by a single photon and in the nuclear three level system a particular hyperfine doublet, as obtained from anticrossing of two nuclear hyperfine levels (Box 2) needs to be used to allow coherent excitation (box 1).

The concepts of coherence and interference were applied to nuclear resonant scattering of synchrotron radiation and a new nuclear interferometer was designed in which one observes the interference between two nuclear resonant scattering amplitudes, one from a reference sample and one from a sample under investigation. From these experiments the hyperfine splitting of the investigated sample can be deduced. This technique has opened a new field of application in the investigation of material properties using nuclear radiation.

The study of coherence phenomena in nuclear radiation led to useful applications also in other fields. For example in nuclear physics the principle of level mixing resonances (LMR) is used for the determination of spins, magnetic and quadrupole moments of exotic nuclei that are produced at a few accelerators in the world.

Finally, lasing and gain without inversion cannot be achieved in nuclear transtions so far, because an adequate pump mechanism is still missing. On the contrary, nuclear level mixing induced transparency has been observed experimentally and can be considered as the nuclear equivalent of optical, electromagnetically induced transparancy. Future investigations in this rich field of research, at the border of nuclear physics, quantum optics, solid state physics and laser physics, will certainly reveal interesting new phenomena and applications for the future.

Acknowledgements

The authors are very grateful to P. Mandel (U.L.B., Belgium), O. Kocharovskaya and Y. Rostovtsev (Texas A&M, USA) for fruitful exchange of ideas on this subject.

References

[1] For recent achievements in this domain of quantum optics, see, for example, S. E. Harris, Physics Today **50**, No 7, 36 (1997); M. Xiao, H. Wang, and D. Goorskey, Optics & Photonics News, p.44, September 2002.

[2] O. Kocharovskaya, Phys. Rep. **219**, 175 (1992).

[3] M. O. Scully, Phys. Rep. **219**, 191 (1992).

[4] C. Liu et al., Nature 409, 490 (2001); D. F. Phillips et al., Phys. Rev. Lett. **86**, 783 (2001); A. B. Matsko et al., Advances in Atomic, Molecular and Optical Physics **46**, 191 (2001).

[5] R. Coussement et al., Phys. Rev. B **54**, 16003 (1996); R. Coussement et al., Hyp. Int. **125**, 113 (2000), R. Callens et al., Phys. Rev. B **65**, 180404 (2002)

[6] J. Odeurs et al., Phys. Rev. B **60**, 7140 (1999).

[7] P. Korecki et al., Phys. Rev. Lett. **79**, 3518 (1997); Phys. Rev. B **59**, 6139 (1999).

[8] H. Frauenfelder, "The Mössbauer effect", Ed. Benjamin 1963, New York

[9] L. A. Rivlin, Hyp. Int. **107**, 57 (1997).

[10] R. Coussement et al., Hyp. Int. **23**, 273 (1985)

[11] G. Neyens et al., Phys. Lett. B **1-2**, 36 (1997)

[12] Proc. of the Int. Gamma Ray Laser conference (GARALAS'97), Hyp. Int. **107** (1997).

[13] G. C. Baldwin, J. C. Solem, and V. I. Goldanskii, Rev. Mod. Phys. **51**, 4 (1981); G. C. Baldwin and J. C. Solem, Laser Phys. **5**, 231, 326 (1995).

[14] C. B. Collins et al., Phys. Rev. Lett. **82**, 695 (1999); J. J. Carroll et al., Hyp. Int. **135**, 3 (2001); C. B. Collins et al., Hyp. Int. **135**, 51 (2001).

[15] P. Walker and G. Dracoulis, Nature **399**, 35 (1999)

[16] U. Köster et al., Nucl. Instr. and Meth. in Phys. Res. B **160**, 528 (2000)

[17] E. S. Fry et al, Phys. Rev. Lett. **70**, 3235 (1993); W. E. van der Veer et al, Phys. Rev. Lett. **70**, 3243 (1993); J. Vanier et al, Phys. Rev. A **58**, 2345 (1998); K. Yamamoto et al, Phys. Rev. A **58**, 2460 (1998);

[18] R. Coussement et al., Phys. Rev. Lett. **71**, 1824 (1993).

[19] R. N.Shakhmuratov et al., Opt. Comm. **179**, 525 (2000); G. Kozyreff, et al., Phys. Rev. A **64**, 013810 (2001).

[20] R. Coussement et al., Phys. Rev. Lett. **89**, 107601 (2002).

[21] J.D. Jackson, "Classical Electrodynamics", 2nd ed. John Wiley and Sons, New York, 1975

Euro coins and the potential risk of nickel allergy

Paul-Guy Fournier[1], Thomas R. Govers[2], and Anne Brun[3]
[1] Laboratoire de Spectroscopie de Translation, Université Paris-Sud, Orsay
[2] Aecono Consulting, Paris
[3] Service Médical du Travail, Université Paris-Sud, Orsay

The concern about nickel in coins

THE choice of design and material to be used in the manufacture of the European common coinage has been the subject of much debate [1]. The incorporation of nickel, in particular, was questioned because of its possible contribution to contact dermatitis: nickel allergy is reported to affect more than 10% of women and several % of men in industrialised countries [2]. A compromise was reached by limiting nickel to the two highest denominations: the 1- and 2€ coins. The surface of both combines a white copper-nickel alloy (Cu75Ni25) with a yellow nickel-brass (Cu75Zn20Ni5), the 1€ having a yellow outer ring and a white centre, the 2€ having a white outer ring and a yellow centre. The six other euro coins do not contain nickel.

nickel allergy is reported to affect more than 10% of women and several % of men in industrialised countries

Several recent articles dealing with leaching experiments or patch tests have renewed attention to the potential allergy risk of the 1- and 2€ pieces [2-4]. The work published by Nestle et al. in the September 12th, 2002, issue of Nature [4], in particular, has been given widespread public coverage, claiming, for instance, that the "euros break EU allergy directive" [5] and that "anybody who is sensitive to nickel may also wish to handle the coins with care" [6]. At time of writing, an internet query with the keywords "euro + nickel + allergy" brought up close to 900 web pages using a popular search engine. Virtually all of these claim that the euro coins represent a danger in regard to nickel allergy, ignoring the fact that the only two nickel-containing euro denominations release *less* nickel upon manipulation than pure-nickel or nickel-alloy coins of comparable size [7].

The 1994 EU "nickel directive" [8] concerns objects designed to come into direct and prolonged contact with the skin. The corresponding normalised test procedure, EN1811 [9], measures the amount of nickel dissolved when the object concerned is immersed in synthetic sweat during one week. When one applies this procedure to the 1- and 2€ coins one detects nickel in amounts comparable to those obtained with other copper-nickel coins and higher than those measured for pure-nickel pieces [2, 4, 10, 11]. These amounts do indeed exceed the 0.5 μg/cm²/week limit of the "nickel directive". But the directive does not apply to coins, and rightly so: interpolating the release rates obtained, taking into account that the manipulation of a coin typically takes less than three seconds rather than a week, one finds numbers that are several orders of magnitude *lower* than what is actually observed in tests that simulate the daily manipulation of coins [11, 7]. The EN1811 test is relevant to long-term solvation upon contact with the skin, but because it does not account for the friction that characterises the manipulation of coins, it is not representative of the amount of nickel transferred to the fingers by the handling of coinage. As anyone can verify when taking a shower, friction is much more efficient in transferring contamination than frictionless solvation.

Manipulation tests

To take friction into account, we have evaluated metal contamination from coins by means of a simple test that simulates daily handling [7]: participating volunteers count a set of coins by transferring them from one polyethylene container to another, and metal contamination sampled by wiping the fingers with cellulose cloths is analysed by inductively-coupled plasma emission spectroscopy (ICP-OES). Details of the procedure can be found in references [7] and [12].

Table 1 summarizes the results of such tests carried out by 3 people counting three sets of 25 used coins each: bi-metallic euros (12 pieces of 1€ and 13 of 2€), Cu75Ni25 copper-nickel coins (2SFr), and pure-nickel 2FF pieces. The first two sets were taken from circulation in a non-industrial environment early 2003, and the last in the beginning of 2002. These 2FF coins had since been stored in a closed polyethylene container. All coins were counted as collected.

	Ambient [7]	1 & 2 €	Cu75Ni25	Ni100
Ni	3.1 ± 0.8	0.31 ± 0.08	0.50 ± 0.16	0.55 ± 0.23
Cu	11.4 ± 3.5	1.95 ± 0.54	1.77 ± 0.54	0.16 ± 0.09
Zn	18.8 ± 5.8	0.29 ± 0.09	0.04 ± 0.03	0.09 ± 0.06
Area 2 faces (cm²)		8.5 & 10.4	11.8	11.0

▲ **Table 1:** Average contamination levels resulting from the manipulation of a single used coin. The second data column lists numbers obtained by counting a set of 12 1€ and 13 2€ pieces; the third column was obtained with 25 2SFr coins, and the last with 25 2FF pieces. All data are expressed in μg. Uncertainties are 90% confidence limits. The first column recalls the average contamination levels found on three fingers as a result of daily activities [7].

Clearly, handling the two nickel-containing euros does transfer significant amounts of nickel to the fingers, but the amounts involved are about 40% *lower* than those resulting from the manipulation of pure-nickel or copper-nickel coins of comparable size. The comparison between the euros and the copper-nickel coins agrees well with the compositions averaged over their respective face areas: Cu75Ni15Zn10 for both bi-metallic euros and Cu75Ni25 for the single-alloy coins. Note that a significant amount of copper is transferred when manipulating pure-nickel francs. We ascribe it to the contamination of the pure-nickel pieces upon contact with copper-containing coins in daily usage.

The contamination transferred to the fingers consists mainly of pre-existing species, rather than compounds generated during manipulation [12]. This is illustrated by fig.1 which shows the decrease in nickel contamination observed upon repeated manipulation of the same used copper-nickel coin (a Swiss 2SFr) or the same used 2€. Handling of a used coin is seen to quite effectively

remove pre-existing contamination by transferring it to the fingers. This transfer becomes less rapid as the number of manipulations increases, because the remaining nickel species are those which are strongest bound to the coin's surface.

The amount of pre-existing metallic species accessible to contaminate the fingers can be evaluated by rubbing the coins to a shiny polish and determining the amount of metal recovered on the "wipes" used to do so [12]. Such polishing reduces contamination upon subsequent handling by more than a factor 10, indicating that it removes more than 90% of accessible pre-existing contamination [12]. The results obtained for several types of nickel containing coins are summarized in table 2.

	2 €	Cu75Ni25	Ni100
Ni	0.48 ± 0.07	0.97 ± 0.37	1.1 ± 0.1
Cu	3.7 ± 0.5	4.0 ± 1.1	1.2 ± 0.7
Zn	0.8 ± 0.2	0.4 ± 0.2	0.2 ± 0.2

▲ **Table 2:** Metal amounts pre-existing on the surface of used coins and accessible to contamination of the fingers by manipulation. The data are expressed in μg per cm^2 and were obtained by dividing the amounts collected when polishing the coins by the geometric surface area of their two faces. The central data column is the average of five different used coins made from Cu75Ni25 copper-nickel alloy. The 2€ and pure-nickel (2FF) data are the average of 60 different coins in each case. Uncertainties are 90% confidence limits.

In this table, the accessible contamination for a single coin has been divided by the geometric surface area of its two faces. The 2€ and the pure-nickel 2FF data are averages pertaining to samples of 60 pieces in each case. The middle column represents the averages of measurements on five different coins made of Cu75Ni25 copper-nickel. This alloy releases essentially the same amount of nickel per unit area as does pure nickel, in spite of its fourfold reduction in nickel content.

When comparing the euro data with the other copper-nickel coins, the accessible amounts of nickel and copper are found to closely reproduce the surface-averaged alloy compositions. The manipulation tests illustrated by table 1 and the accessibility measurements of table 2 are fully coherent, and neither set of data shows any evidence for enhanced nickel release due to the bimetallic structure of the 1- and 2€ coins, contrary to the strong galvanic effect reported in the case of immersion tests [4,7].

Patch tests

As nickel allergy results from penetration of the skin by nickel ions [13, 14], the question arises what portion of nickel contamination, once transferred to the fingers, will be dissolved before being removed by washing or rubbing hands. We have examined the dissolution rates upon contact with the skin by means of "patch" tests analogous to those employed by Aberer and Kränke [3]. In the present case, we have replaced visual evaluation by quantified measurement of metal release using the same sampling and analysis procedure as in the manipulation tests. To obtain data representative of the coin constituents, the different pieces investigated were previously polished to remove superficial contamination.

Two patch tests were carried out, each with 8 different coins, these being left taped to the skin during 24 and 72 hours, respectively. Subsequently, the tapes and coins were carefully removed, and the imprint on the skin of each individual coin was thoroughly rubbed, each time using fresh cellulose "wipes" which were separately stored in closed polyethylene containers. This sampling procedure was carried out at the University health centre, under medical supervision.

Figure 2 illustrates the imprints observed after 72 h skin contact of four different coins, identified in the photograph. There are no obvious visual differences between the various pieces, except, perhaps, for the stronger mark left by the copper-nickel Swiss 2SFr as compared to that due to the 2€ coin. The mark left by the nickel-free 0.50€ piece (Cu89Al5Zn5Sn1) is visually quite similar to that of the three other coins, made of nickel-alloys, illustrating that much of the observed coloration is due to copper rather than to nickel. There is no resemblance at all to the spectacular visual difference between the Swiss franc and the euro observed upon long-term immersion in artificial sweat [4, 15].

In the laboratory, ICP-OES analysis was applied to the "wipes" used to rub the imprints on the arm and also to those employed for sampling metals released on the surfaces of the coins that had been in contact with the skin. The results are summarised in fig.3, where the sum of the metals collected on the skin and on the coins are reported as release rates per cm^2 and per week. Expressed in this fashion, the results from the 24 h experiment, indicated by an asterisk*, and from the 72 h patch test show little difference, indicating that there are no important saturation effects in spite of the limited amount of sweat available to dissolve into.

The data demonstrate a remarkable consistency between coins of similar composition and a close correlation with the surface-averaged proportion of the metals examined. The Swiss, American, and Swedish coins, as well as for the British 10p are all made of Cu75Ni25 copper-nickel, and for both constituents the release rates per cm^2 too are very similar. The nickel release averages between 20 and 30 μg of nickel per cm^2/week, the area considered being that of one face of the coin. This is about twice as much as the results obtained with the pure-nickel 1FF pieces, in qualitative agreement with prolonged immersion experiments in artificial sweat, which yield an even larger increase in nickel release from copper-nickel as compared to pure nickel [2,4,10,11].

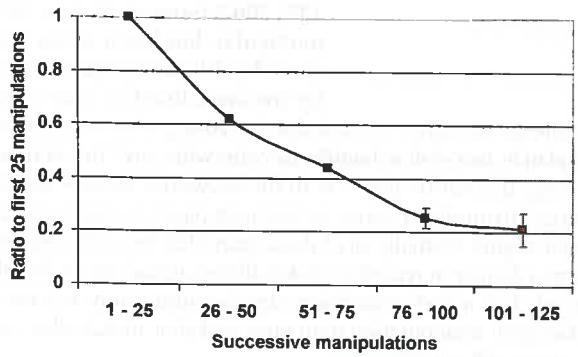

▲ **Fig. 1:** Evolution of nickel contamination upon repeated manipulation of the same used coin, whereby the fingers are wiped for metal analysis after each sequence of 25 manipulations. The data are reported as ratios to the quantities obtained for the first sequence, and are the averages of the ratios obtained with used 2€ coins and used copper-nickel pieces. The error bars indicate the spread between the two types of coins.

▲ **Fig. 2:** Imprints visible just after removing coins that had been taped to the skin during 72 hours.

The nickel release rates obtained with the 1- and 2€ coins are *lower* than those of the single-alloy pieces, and show no evidence of strong galvanic enhancement due to their bi-metallic structure. In fact, the euro data correlate well with the behaviour of the two alloys employed: the white half of the euros' surface has the same composition as the six copper-nickel coins just mentioned, and the other (yellow) half closely resembles the 1£ coin, made of Cu70Ni5.5Zn24.5 nickel-brass. As fig.3 shows, the euro coin results indeed fall in between the copper-nickel and nickel-brass data.

The 0.50€ coin, consisting of nickel-free "Nordic Gold", releases copper slightly higher in proportion to its copper content than the copper-nickel coins, indicating a somewhat lower corrosion resistance upon contact with human sweat. Its nickel release rate is small, about 3 µg per cm² and per week, but significantly higher than can be ascribed to nickel impurity in its constituents. This contamination probably results from contact with the nickel-containing 1- and 2€ pieces in daily usage. As the coins were polished at the onset of the present patch tests, the persistence of this metallic cross-contamination reflects relatively strong adhesion to the coin's surface. An analogous explanation probably applies to the copper observed on the pure-nickel French franc and to the zinc on the 50 öre and on the US coins.

Allergic risk

We have shown above that in experiments representative of the handling of coins, the nickel-containing 1€ and 2€ coins behave very similarly to single-alloy copper-nickel pieces, in regard both to contamination transfer by friction and to dissolution upon contact with the skin. It is therefore reasonable to assume that the nature of the contamination transferred to the fingers is similar in both cases. When comparing these two euro pieces to other copper-nickel coins, the relative risk of nickel allergy should in that case be in proportion to the amounts of nickel transferred by manipulation. This amount is typically 40% lower with the 1- and 2€ pieces, as reported in table 1 and in ref. [7], suggesting that the two nickel-containing euros represent a lesser risk of nickel allergy than Cu75Ni25 copper-nickel coins of similar size.

The comparison may be less straightforward when comparing the euros with pure-nickel coins, as the fraction of transferred nickel that dissolves before washing or rubbing hands may be different. As illustrated by fig.3, the nickel dissolution rate of the Cu75Ni25 alloy upon contact with the skin is about twice as high as that of pure nickel. If for both the copper-nickel and pure-nickel coins *all* of the transferred contamination consists of slowly dissolving compounds or particles, this factor of two will compensate the twofold reduction in the amount of nickel transferred to the fingers (table 1). The allergic risk of the 1- and 2€ coins should then be comparable to that of pure-nickel pieces of similar size. If all contamination from pure nickel coins dissolves slowly, while that from copper-nickel alloys contains a rapidly dissolving component, the 1- and 2€ pieces may represent a higher risk than pure-nickel coins. This rather surprising conclusion would of course equally apply to any other copper-nickel coin.

> A more precise assessment of relative allergy risks requires further investigation

A more precise assessment of relative allergy risks requires further investigation into the nature and solubility rates of metallic contamination resulting from the handling of coins. Preliminary results obtained by energy-dispersive electron-beam microscopy confirm the contribution of particulate matter. This is illustrated by fig.4, which shows micrographs of conductive tape that has been in contact with the border area across the two alloys of a 2€

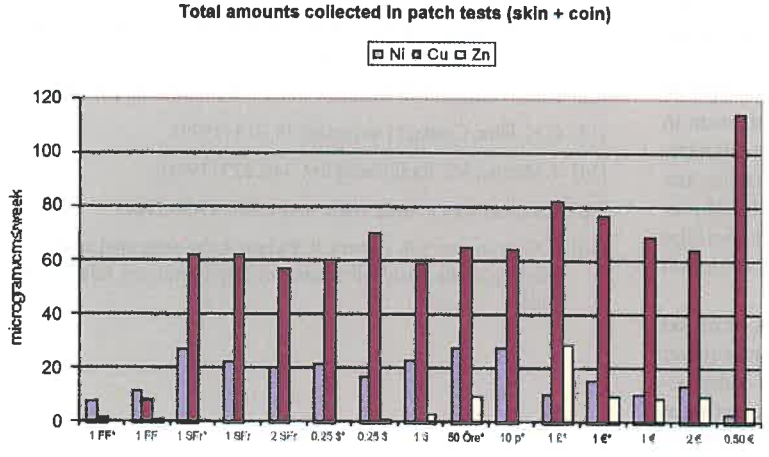

◀ **Fig. 3:** Metal release rates determined by taping polished coins to the skin for a duration of 24 h (data labelled with an asterisk*) or 72 h. They were obtained by adding the metals sampled from the imprints left on the skin and those from the face of the coin that had been in contact with the skin. Their respective contributions were in a ratio of about 3 to 1. The release rates are expressed in µg per cm² and per week, where the surface considered is the geometric area of one face of the coin.

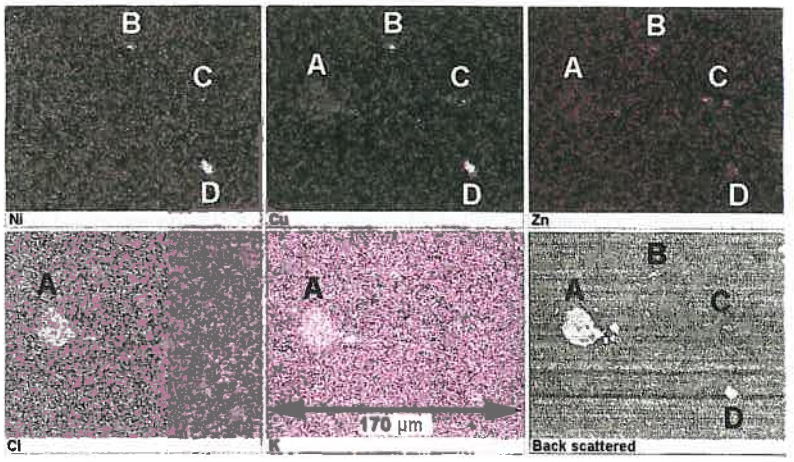

◀ Fig. 4: Backscattered electron scan and secondary electron micrographs of adhesive tape that has been in contact with the border area encompassing the two different alloys of a 2€ coin (Cu75Ni25 and Cu75Zn20Ni5). The compositions of the labelled features are: A = Na 37%, K 25%, Ca 3.5%, Cl 32%; B and D = Cu 76%, Ni 23.5%; C = 75.5%, Zn 19.5%, Ni 4.3%. Feature A is probably a skin and/or sweat residue, while B, C and D are metallic particles with the same composition as the coin's alloys.

piece. Several µm-size particles are seen B, C and D, whose composition closely matches that of the coin's Cu75Ni25 and Cu75Zn20Ni5 alloys. The largest object, labelled "A", is probably a sweat and/or skin residue [16].

Conclusions

The two nickel-containing 1- and 2€ coins do contribute to the contamination of the fingers by nickel and this contamination can be reliably evaluated by manipulation tests. The amounts of metallic species that pre-exist on the surface of coins and which represent a reservoir accessible to contamination by handling, can be quantified by polishing the pieces and analysing the metals thus sampled. The amount of nickel accessible on pure-nickel or Cu75Ni25 copper-nickel surfaces is of the order of 1 µg/cm^2, while it represents about 0.5 µg/cm^2 averaged over the surface of the bi-metallic euro coins. Typically, a single manipulation of a used nickel or copper-nickel coin with a face area of about 10 cm^2 releases ≈ 0.5 µg of nickel, while ≈ 0.3 µg is transferred to the fingers when handling a 1- or 2€ piece. Taking into account published exposure thresholds [14] these quantities imply that skin concentrations sufficient to provoke allergic reactions will be reached upon manipulation of several hundred coins. Compulsive manipulation of a same coin is unlikely to reach the non-occluded threshold of 15 µg/cm^2 [14], since the contribution of each piece is limited by the accessible "reservoir", which is of the order of 1 µg per coin, distributed over 10 cm^2 finger area.

When taped to the skin, even previously polished 1- and 2€ coins will provoke, after several hours, a nickel concentration in excess of 1 µg/cm^2. In prolonged patch tests, these coins will therefore produce allergic reactions with sensitized people, just like any other nickel– or copper-nickel piece, as clearly shown by Aberer and Kränke [3]. While such tests confirm that the bi-metallic euros behave similarly to other copper-nickel pieces, they do *not* represent evidence for an increased allergic risk.

It is therefore quite legitimate to claim that the risk of nickel allergy due to the manipulation of coins could have been further reduced by not incorporating any nickel in the surface composition of the common currency. There is, however, no pertinent evidence to support the much publicised notion that the introduction of the euro has increased the risk of nickel allergy.

Acknowledgments

We are indebted to the Comité Mixte Inter-Universitaire Franco-Marocain (Grant AI 99/186F/SM and Grant MA 02/39), to Scientartphie Environnement, and to the Marionnaud company for financial support.

References

[1] A.L.Friedberg, The Numismatist, April 2002, 384.

[2] C. Lidén, S. Carter, Contact Dermatitis 44, 160 (2001).

[3] W. Aberer, B. Kränke, British J. Dermatology 146, 155 (2002).

[4] F.O. Nestle, H. Speidel, M.O. Speidel, Nature 419, 132(2002).

[5] C. Westney, Nature Science Update, Sept. 12,(2002)

[6] The Economist, Sept. 14, 2002.

[7] P.-G. Fournier, T.R. Govers, J. Fournier, M. Abadi, C.R. Physique 3, 749 (2002).

[8] European Parliament and Council Directive 94/27/EEC, JO CE L 188, 1 (1994).

[9] European Committee for Standardisation (CEN), JO CE C 205, 5 (1999): EN 1810 (1998), EN 1811 (1998), EN 12472 (1998).

[10] N.B. Pedersen, S. Fregert, P. Brodelius, B. Gruvberger, Acta Dermatovener 54, 231 (1974).

[11] P.-G. Fournier, T.R. Govers, M. Abani, H. Boughaleb, M. Monkade, Phys. Chem. News 6, 82 (2002).

[12] P.-G. Fournier, T.R. Govers, Contact Dermatitis 48, 181 (2003).

[13] G.N. Flint, Contact Dermatitis 39, 213 (1998).

[14] T. Menne, Sci. Total Environm. 148, 275 (1994).

[15] J. Stephenson, J. Amer. Med. Assoc. 288, 1708 (2002).

[16] P.-G. Fournier, T.R. Govers, R. Pichon, to be presented at the General Meeting of the Société Française de Physique, Lyon, July 7 – 10, 2003.

Synchrotron Radiation opens a new series of EPS seminars

François Bourgeois, Chairman of the EPS Technology Group

THE first EPS Technology Foresight seminar took place on Tuesday 24 June in Munich in the framework of the Laser 2003 exhibition. Entitled "Synchrotron Radiation and Free Electron Lasers", it was the first in a series of seminars that are being organized as part of renowned industrial exhibitions and conferences. These seminars present and explain in simple terms new advances in physics, which may be of relevance for industry and the market place in the coming few years.

The outstanding high resolution and fast data collection characteristics of the X-ray beams provided by Synchrotron Radiation (SR) sources have made them essential for collecting high quality diffraction data. They have a wide range of applications including biocrystallography for drug design, real-time analysis of the growth of crystals, or trace element analysis on silicon wafers. Free Electron Lasers (FELs) generate tuneable, coherent, high-power sub-nanosecond radiation pulses, currently spanning wavelengths from millimetre to visible, ultraviolet and even X-rays.

Speakers were chosen among leading experts from SR laboratories and Industry. They gave an overview of the SR and FEL technologies and the main benefits that industry, biology, and medicine might draw from their use in the years to come.

Welcome address by the EPS President

Dr Martin Huber, President of the European Physical Society (EPS), welcomed the participants, 28 members of European industry who were invited to attend. He said that the EPS was starting there an activity, through which physicists can provide a worthwhile, even useful service to Industry.

The European Physical Society was founded in 1968 as a learned society, and for a few decades the focus was on the academic pursuit of physics. Times have changed and there is nowadays a justified need for a closer connection and an improved exchange of knowledge between Academia and Industry. Society at large also supports the view that basic science findings be put to use where appropriate and without delay. The EPS is therefore willing to contribute to shortening the time that elapses from the moment when a relevant research result is found and established, until it is actually applied in the market place. To this end, Industry should be better informed of the latest achievements in physics, and of those instruments and procedures that are likely to find an application in the development of products for the market. It is believed that the EPS can be of help to Industry in identifying some of its needs and goals in terms of applied research. Dr Huber noted in this respect that a visit to the Laser 2003 Exhibition gave a stern lesson to those journalists who in the early 1960s belittled the laser as "the solution to a problem that didn't exist."

M. Huber said that he was very interested in finding out from the participants what they perceived as being helpful for Industry. He noted that as a former member of the Scientific Directorate of the European Space Agency, 85% of their programme funds were spent in technologically advanced work in Industry. He was, however, aware that Technology Transfer had many more facets, and that there were other ways to foster a fruitful collaboration between Physics and Industry.

Prior to giving the floor to the six SR experts, Dr Huber said that the EPS was pleased to acknowledge the help and support from the CERN[1], DESY[2], Elettra[3], ESRF[4] and PSI[5] laboratories in the organization of this seminar. He thanked the speakers for sparing some of their valuable time in this endeavour, which, he was convinced, would be a success.

Brief account of the six talks

Managing and Scientific Director of the Elettra Synchrotron Light Laboratory in Trieste, Italy, Professor Massimo Altarelli gave the first talk entitled "The Quest for High Brilliance: Synchrotron Light Sources from the 3rd to the 4th Generation". His contribution included an overview of the physics and the salient properties of synchrotron radiation. There are about 50 synchrotron light sources worldwide of which 10 belong to the most recent (and most brilliant) generation. Their unique features and broad scientific applications were presented. The next generation sources of ultraviolet and X-rays (Free-electron Lasers, Energy Recovery Linacs) with full spatial coherence were also presented. Soft and hard X-rays with high average brilliance will be achieved with 4th generation sources. High peak brilliance, and sub-ps (down to ~ 50 fs) pulses can open new perspectives to the study of the structure and properties of molecules, biomolecules and materials.

The second talk entitled "Synchrotron X-Ray Imaging, a Tool for Industrial Applications" was given by Dr. José Baruchel, Head of the X-ray Imaging Group at ESRF. X-ray imaging started over a century ago. For several decades its only form was absorption radiography. In the 1960s Bragg-diffraction imaging (X-ray topography) developed into practical use for characterization of crystals for the microelectronics industry.

The modern synchrotron radiation (SR) sources, coupled with improvements in the detection, optics, and computer power, has allowed the emergence of several new forms of X-ray imaging. These include: Scanning Imaging, with element chemical state speciation, developed in connection with the availability of very efficient lenses; Microtomography (three-dimensional imaging (see Figure 1), with a spatial resolution in the micron range) that allows a wide range of topics, including the deformation of foams or the structure of cosmetics, to be addressed. The very small size of SR sources now also makes possible, through the coherence of the X-ray beams, the use of phase contrast imaging, which has proved to be invaluable when studying, for instance, the porosity of materials, the *in situ* damage of composites, or the structure of

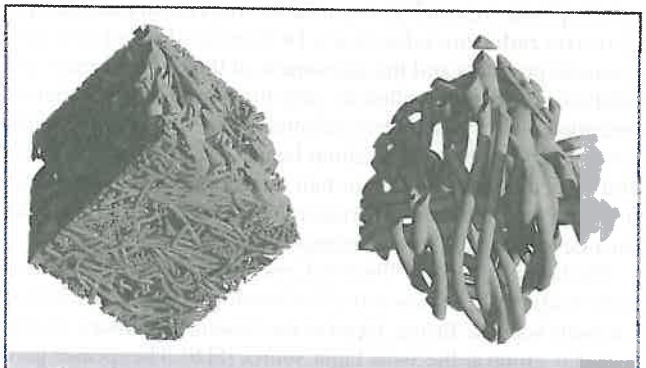

▲ **Fig. 1:** Microtomography combined with image processing allows for the identification of large fibres in a sample of felt.

Fig. 2: The speakers enjoying an informal Bavarian drink at the end of the seminar; left to right: M. Altarelli, Å. Kvick, J. Baruchel, J. Doucet, C. Schulze-Briese, J. Trenkler and F. Bourgeois.

micro-heterogeneous compounds. These new capabilities were illustrated by applications to industrial problems.

In the ensuing talk entitled "Novel Materials Science Studies using Synchrotron Radiation", Professor Åke Kvick, Head of the materials science group at ESRF, reminded the audience that the knowledge of structure-property relationships of materials is the basis for the rational design of new materials. The use of the unique properties of synchrotron radiation i.e. extreme brilliance, tenability, microfocusing and coherence was shown and discussed in a series of studies of materials ranging from metals to polymers.

The fourth speaker was Dr Johann Trenkler who is carrying out research on the development of large-scale Extreme Ultraviolet Lithography (EUVL) multilayers with atomic precision at the Carl Zeiss SMT AG in Oberkochen, Germany. EUVL using 13 nm radiation will be the next generation lithography technology to achieve structural sizes below 50 nm, when reflective optics will replace current refractive systems. His talk gave a thorough overview of the EUVL programme at Carl Zeiss SMT AG with special focus on the stringent demands on the mirror fabrication and coating technology. He showed not only that a mirror metrology is fully at hand to qualify the surface shape and surface finish of the mirrors but also that soft-X-ray synchrotron radiation as well as hard X-rays are utilized to determine the atomic precision of the EUV multilayers. Special attention was devoted to the Micro Exposure Tool (MET), which consists of EUV optics. Resist images with a resolution down to 35 nm (!) could be taken when the MET was operated at the PTB at the Bessy2 synchrotron in Berlin.

The ensuing talk, "Synchrotron-Radiation-Based Techniques and the Cosmetics Industry" was given by Dr Jean Doucet, Head of a biophysics research group at LURE, the French national synchrotron radiation laboratory. Dr Doucet showed how new cosmetic products and the assessment of their effectiveness and safety for consumers called for very high-performance characterization tools. Synchrotron-radiation-based techniques provide new in-depth information about beauty creams, hair products and their tolerance by skin or hair. Many cosmetics companies benefit from modern synchrotron light sources for optimizing their developments. Several examples were given.

The last talk, entitled "Protein Crystallography with Synchrotron Radiation: Science and Technology" was given by Dr Clemens Schulze-Briese, Head of the Macromolecular Crystallography group at the Swiss Light Source (SLS). The speaker gave an overview of the advantages of the use of synchrotron radiation in the field of protein crystallography (PX), both for challenging projects as well as for high-throughput structural genomics and drug design. This was illustrated by recent scientific highlights and the plans for a second PX beamline at the Swiss Light Source for the Swiss pharmaceutical industry and the Max-Planck Gesellschaft.

Outcome and future subjects

The replies to an evaluation questionnaire filled in by the participants at the end of the meeting confirmed the excellence of the talks. All speakers were highly rated and some of the participants saw opportunities for their business. Fruitful discussions took place during refreshments at the end of the day (see Figure 2).

Future seminars will be organised in the framework of conferences and exhibitions that are well attended by Industry. Other seminar topics will be chosen in collaboration with the network of EPS industrial contacts, and interested parties are welcome to join this network. In addition to these seminars *EuropysicsNews* has the intention to feature from now on more reports of relevance for Industry. To begin with, most of the talks given at this Synchrotron Radiation and Free Electron Lasers seminar will appear as articles in the 2004 issues of *EuropysicsNews*.

Footnotes

[1] European Organization for Nuclear Research, http://www.cern.ch

[2] Deutsches Elektronen-Synchrotron (D), http://www.desy.de

[3] Elettra Synchrotron Light Laboratory, Trieste (IT), http://www.elettra.trieste.it

[4] European Synchrotron Radiation Facility, Grenoble (FR), http://www.esrf.fr

[5] Paul Scherrer Institute, Villigen (CH), http://www.psi.ch

Universities in the Europe of Knowledge

THE EPS, in addition to many other large European learned societies (EMRS, EURO-Case, FEBS...) was invited to attend a workshop on the subject of the Europe of Knowledge in 2020. The European Commission is organising a conference on this topic in Liège, Belgium (26-28 April 2004). The workshop is on in a series to help define the programme and speakers at the conference to address the issues that are of importance not only to the EC, but to the scientists themselves. The interest in the role of universities fall within the policy context of the ERA, the Bologna process and the EC Communication in 2003 on the role of the universities in the Europe of knowledge. The workshop analysed the responses by from the scientific community to this communication, the need to maintain and increase basic research facilities and funding in universities, and what links with transfer of technology could and should be established. The EPS replied to the consultation, and the full text of the EC communication can be found at http://europa.eu.int/eur-lex/en/com/cnc/2003/com2003_0058en01.pdf. The full text of the replies should be online shortly.

EPL moves to Mulhouse

FOLLOWING the decision of the Europhysics Letters Board of Directors, the EPL Editorial Offices are moving to Mulhouse. The movers arrived early in the morning of 24 September, bringing the files and equipment to install the editorial offices. K. Degenstein and Y. Sobieski, the 2 new assistant editors are working hard to organise the new office, and have been instrumental in coordinating the move.

NEST

SOMETIMES called the eighth thematic priority, the New and Emerging Science and Technologies programme in FP6 is specifically designed to search, finance and coordinate high risk, and eventually high return research in fields that either fall outside, or cut across the 7 thematic priorities of FP6. (see http://www.cordis.lu/fp6/activities.htm for an overview of FP6). NEST has two bottom up initiatives. The first, ADVENTURE, is for research in emerging areas of knowledge and on future technologies. The second, INSIGHT, is for research to rapidly assess new discoveries or newly observed phenomena which may indicate emerging risks or problems. Specific support actions focussed on the conceptual and practical questions associated with NEST research domains can also be funded. The first calls for funding under these bottom up initiatives is open until 22 October 2003. Finally, NEST also has focussed actions through PATHFINDER, which define specific areas in which research may be funded. The first call should be made October 2003, with a deadline for applications in 2004.

Lise Meitner Prize

THE Nuclear Physics Board of the EPS invites nominations for the year 2004 for the "Lise Meitner Prize". The award will be made to one or several individuals for outstanding work in the fields of experimental, theoretical or applied nuclear science. The Board would welcome proposals which represent the breath and strength of European nuclear sciences.

For nomination form and more detailed information see: http://www.kvi.nl/~eps_np

Nominations will be treated in confidence and although they will be acknowledged there will be no further communication. Nominations should be sent to:

Selection Committee LM Prize
Chairman Prof. Ronald C. Johnson,
Department of Physics, School of Physics and Chemistry,
University of Surrey
Guildford, Surrey
GU2 7XH, United Kingdom
Phone: +44 (0)1483 879375
Fax: +44 (0)1483 876781
E-mail: R.Johnson@surrey.ac.uk

The deadline for the submission of the proposals is 10.01.2004.

BELOW is a list of EPS Europhysics Conferences, and EPS Sponsored Conferences. Europhysics Conferences are organised by EPS Divisions and Groups. Sponsored Conferences have been reviewed by experts in the field following application, and based on criteria such as timeliness and topical coverage, are considered to merit EPS sponsorship.

2004 EUROPHYSICS CONFERENCES

Ninth European Particle Accelerator Conference (EPAC 2004)
05–09 July 2004, Lucerne Centre, Switzerland
contact Prof. Hans-Arno Synal
Chairman of the LOC
PSI ETH Hönggerberg Bldg. HPK
CH-8093 Zurich
tel +41 1 633 2027 **fax** +41 1 633 1067
email Synal@phys.ethz.ch
contact Mrs Christine Petit-Jean-Genaz
EPAC Conference Coordinator
CERN-AC
CH-1211 Geneve 23
tel +41 22 767 32 75 **fax** +41 22 767 94 60
email Christine.Petit-Jean-Genaz@cern.ch
web www.epac04.ch

The 20th General Conference of the Condensed Matter Division of European Physical Society (CMD20)
19–23 July 2004, Congress Center, Prague, Czech Republic
contact Dr. Frantisek Chmelik
Charles University Metal Physics Dept.
Faculty of Mathematics & Physics
Ke Karlovu 5 12116 Praha 2 Czech Republic
tel +420 2219 11358 **fax** +420 2219 11490
email sech@mag.mff.cuni.cz
web http://cmd.karlov.mff.cuni.cz/CMD/

Conference on Computational Physics: CCP 2004
01–04 September 2004, Conference Center
Magazzini del Cotone, Genova (Italy)
contact Prof. Giovanni Ciccotti
Dipartimento di Fisica
Università "La Sapienza"
P.zzale A. Moro, 2
00185 Roma, Italy
tel +39 06 49 91 43 78 **fax** +39 06 49 57 697
email Giovanni.ciccotti@roma1.infn.it

12th International Conference on the Physics of Highly Charged Ions (HCI 2004)
06–10 September 2004, Vilnius University (Lithuania)
contact Dr. Andrius Bernotas
Vilnius University
Research Institute of Theoretical Physics & Astronomy
A. Gostauto 12
2600 Vilnius, Lithuania
tel/fax +370 5 212 53 61
email hci2004@itpa.lt
web www.itpa.lt/hci2004

2004 SPONSORED CONFERENCES

Xth Vienna Conference on Instrumentation
16–21 February 2004, University of Technology, Vienna (Austria)
contact Professor Meinhard Regler
Institute of High Energy Physics of the Austrian Academy of Sciences
Nikolsdorfergasse 18
A-1050 Vienna, Austria
tel +43 1 544 73 28 41 **fax** +43 1 544 73 28 54
emails vci@hephy.oeaw.ac.at or meinhard.regler@oeaw.ac.at
web http://vci.oeaw.ac.at

Coupled Map Lattices 2004
21 June–02 July 2004, Institut Henri Poincaré, Paris (France)
contact Prof. J-R. Chazottes
Ecole Polytechnique Centre de Physique Théorique
91128 Palaiseau Cedex, France
tel +33 169 333 542 **fax** +33 169 333 008
email jeanrene@cpht.polytechnique.fr
Prof. B. Fernandez
CNRS Luminy Case 907
Centre de Physique Théorique
13288 Marseille Cedex 09 France
tel +33 491 269 549 **fax** +33 491 269 553
email bastien@cpt.univ-mrs.fr
web www.cpht.polytechnique.fr/cpth/chazottes/ihp2004.html

The forthcoming deadline for applications for magnet time allocation (February to July 2004) at the

GRENOBLE HIGH MAGNETIC FIELD LABORATORY

is **November 14th, 2003**

Scientists of EU countries and Associated States* are entitled to apply under the European Programme to obtain a financial support according to rules defined by the EC. Application forms are available on request.

* Bulgaria, Czech Republic, Republic of Cyprus, Estonia, Hungary, Iceland, Israel, Latvia, Liechtenstein, Lithuania, Norway, Poland, Romania, Slovakia, Slovenia.

Please contact:

E. Mossang
Laboratoire des Champs Magnétiques Intenses,
MPIFKF - CNRS
B.P. 166
38042 Grenoble Cedex 9 FRANCE
Tel. : 33- 4.76.88.74.87
Fax : 33- 4.76.85.56.10
e-mail : mossang@grenoble.cnrs.fr

UNIVERSITÉ DE GENÈVE

The **FACULTY OF SCIENCES** has an opening for a position of

Full or Associate Professor (Professeur-e ordinaire ou adjoint-e)

in Theoretical Statistical Physics

Responsabilities: this is a full time appointment comprising 6 hours of teaching per week as well as research activities in the area of modern methods and problems in statistical physics.

Degree requirements: Ph.D or equivalent.

Beginning: October 1, 2005 or as agreed.

Applications, including a curriculum vitae, a list of publications and a list of references are to be sent by March 1st, 2004 to the Dean of the Faculty of Sciences, 30, Quai Ernest Ansermet, CH-1211 Geneva 4 (Switzerland), where further information concerning job description and working conditions can be obtained.

Applications from women are particularly welcomed.

Postdoctoral fellowships at the Niels Bohr Institute University of Copenhagen

The Niels Bohr Institute is part of the Physics Department of Copenhagen University (NBIfAFG) and has active theoretical and experimental research programs in theoretical high energy physics, nuclear physics, and the physics of nonlinear and complex systems. The Institute shares building facilities with the independent Nordic research Institute, Nordita and there is considerable scientific collaboration with that Institute. More information about the Institute is available at http://www.nbi.dk/.

Applicants should submit a curriculum vitae, list of publications, a statement of their research interests and goals, and arrange for 2-3 letters of reference, to be sent to

Niels Bohr Institute - c/o Ulla Holm - Blegdamsvej 17
DK-2100 Copenhagen - Denmark.
Fax +45 35325400

Applications for the academic year 2004/2005 should arrive before 12 December 2003.

Enquiries can be directed to postdoc@nbi.dk

Laboratoire Kastler Brossel
École Normale Supérieure, Université Pierre et Marie Curie and CNRS

Paris, France

A full professor position in Atomic Physics or Quantum Optics is likely to open next year at the laboratoire Kastler Brossel.

Experimental Quantum Physics

Research: The Kastler Brossel Laboratory is looking for a young professor to start a new experimental team. This team should integrate harmoniously in the research activity of the laboratory, centered on fundamental aspects of light-matter interaction, and complement existing activities. No particular subject is imposed. Among others, possible subjects are applications of atom cooling by lasers to atom chips, measurements of fundamental quantities, quantum information, complex quantum systems. The applicants should have a strong experience in scientific research, be able to perform an independent research activity by leading a research team working on original themes at the forefront of physics.

Teaching: The applicants should be able to teach in French at all university levels, including experimental teaching. They should be willing to contribute to the renovation of quantum mechanics courses.

Specific details:

In the French university system, applicants to professorship must submit a non-committing application at the national level in order to be registered in a "qualification list". Deadline for registration is usually early October or end of September. The decision on the availability position has already been taken at the Physics Department level (UFR), but the final decision for position opening will be made in early February. Interested applicants should therefore register to the qualification list in time.

Interested persons should get in contact with Franck Laloë, Director of the Laboratory (laloe@ens.fr, +33-1 47 07 54 13)

EDP SCIENCES

An Internationa Scientific Publishe

- Agronomie
- Animal Research
- Annals of Forest Science
- Annales de Physique
- Apidologie
- Astronomy & Astrophysics
- Environmental Biosafety Research
- European Astronomical Society - Publications Series
- European Physical Journal (The) - Applied Physics
- European Physical Journal B (The)
- European Physical Journal D (The)
- European Physical Journal E (The)
- ESAIM: Control Optimisation and Calculus of Variations (COCV)
- ESAIM: Mathematical Modelling and Numerical Analysis (M²AN)
- ESAIM: Probability and Statistics (P&S)
- ESAIM: Proceedings (PROC.)
- Europhysics Letters
- Europhysics News
- Fruits
- Genetics Selection Evolution
- Journal sur l'enseignement des sciences et technologies de l'information et des systèmes
- Journal de Physique IV - Proceedings
- Lait (Le)
- Quadrature
- RAIRO: Operations Research
- RAIRO: Theoretical Informatics and Applications
- Radioprotection
- Revue de l'Électricité et de l'Électronique
- Reproduction Nutrition Development
- Revue de Métallurgie
- Veterinary Research

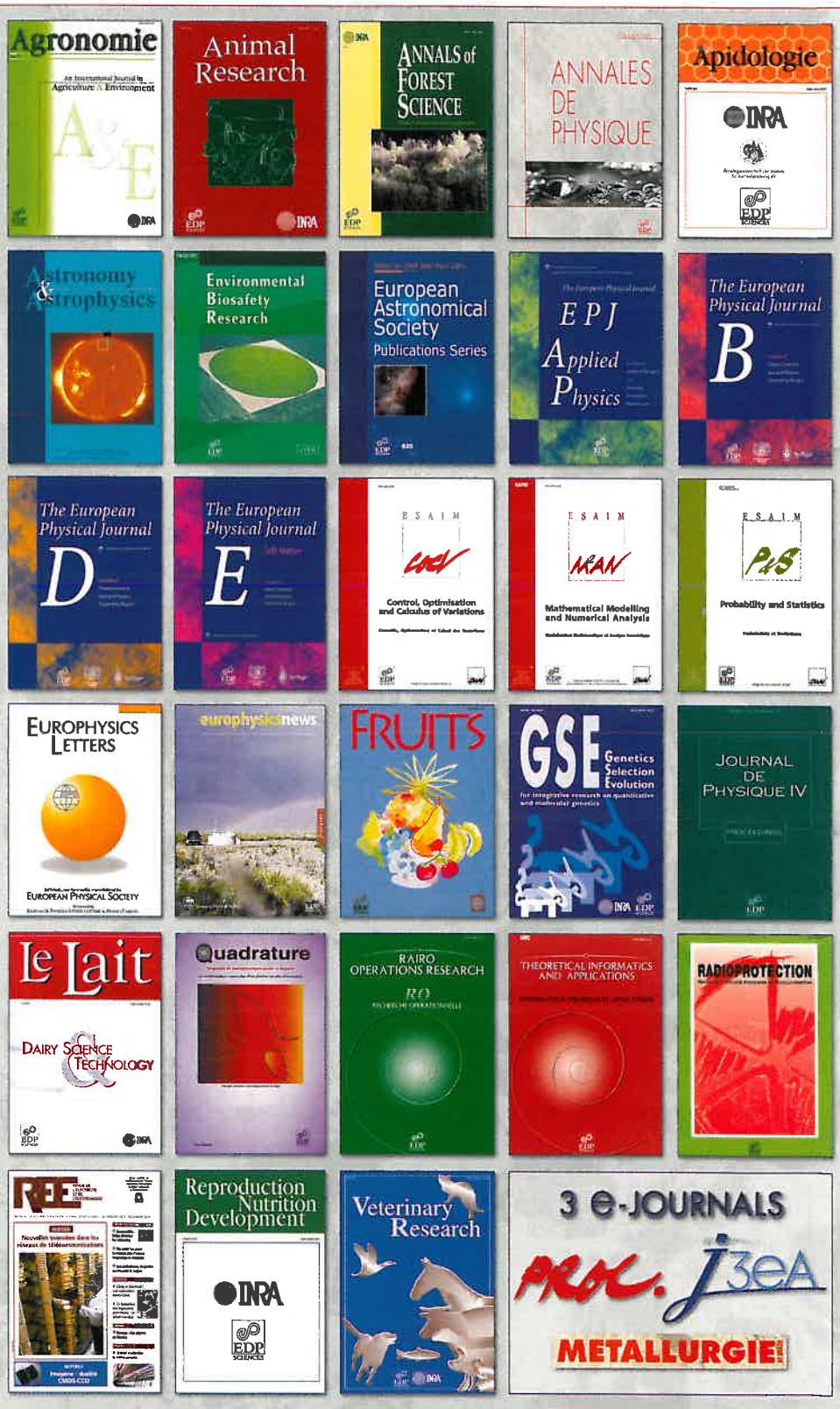

EDP Sciences : 17, avenue du Hoggar • BP 112 • P.A. de Courtabœuf • 91944 Les Ulis Cedex A • France
Tel. 33 (0)1 69 18 75 75 • Fax 33 (0)1 69 86 06 78 • subscribers@edpsciences.org • http://www.edpsciences.org